Università degli Studi di Cagliari

SCUOLA DI DOTTORATO IN

Tossicologia - Oncologia e Patologia Molecolare

XXIII ciclo

DETERMINATION OF HIPPO PATHWAY INVOLVEMENT IN TCPOBOP-INDUCED PROLIFERATION IN NORMAL LIVER AND HEPATOCELLULAR CARCINOMA

Settore Scientifico Disciplinare di Afferenza: MED/04

Presentata da: Christian Saliba

Direttore: Prof. Gaetano Di Chiara

Relatore: Prof.ssa Giovanna Maria Ledda

Esame Finale Anno Accademico 2009-2010

ACKNOWLEDGEMENTS

I would like to express my sincere appreciation to Prof. Amedeo Columbano and Prof. Giovanna Maria Ledda for giving me this opportunity. I owe them my intellectual development during these years.

I am also deeply grateful to Prof. Michael Schwarz and Dr. Albert Braeuning from the University of Tübingen for accepting me in their laboratory to be able to perform the mutation analysis for the accomplishment of this thesis.

I am greatly indebted to Assistant Prof. Monica Pibiri for her enlightened guidance and constructive suggestions during the correction of this dissertation. Her conceptual insights into this work have been invaluable.

I would like to heartfully thank Dr. Roberto Loi for his advice on the mutation analysis, Dr. Vera P. Leoni for her support with the RT-PCR analysis and Dr. Andrea Perra for his assistance with the immunohistochemical staining.

I would also like to thank all my colleagues, whose friendship has helped me strive throughout my years spent at the University of Cagliari.

Finally a word of thanks goes also to my parents, my parents-in-law and my girlfriend for their unconditional and unwavering understanding, support, and encouragement throughout my study.

“In times of great change (which is always), learners inherit the earth, while the learned find themselves beautifully equipped for a world that no longer exists.”

Eric Hoffer (1902 - 1983), philosopher

CONTENTS

ABSTRACT

Recenti studi condotti su modelli di topi transgenici hanno evidenziato che nei mammiferi la regolazione delle dimensioni di un organo è controllata dalla cascata chinasica *Hippo pathway*, che sopprime la crescita antagonizzando il co-attivatore trascrizionale *Yes-associated protein* (YAP). Lo scopo di questo studio è stato quello di indagare se: la *Hippo pathway* gioca un ruolo critico nell'arresto della crescita del fegato indotta dalla somministrazione di dosi ripetute del mitogeno 1,4-bis[2-(3,5-dicloropiridilossi)]benzene (TCPOBOP), un'agonista del recettore nucleare *constitutive androstane receptor* (CAR); la disregolazione di questa *pathway* è coinvolta nello sviluppo dell'epatocarcinoma (HCC), indotto in seguito al trattamento con una singola dose di dietilnitrosamina (DENA) e seguito dalla somministrazione di dosi ripetute del TCPOBOP. I risultati di questo studio hanno dimostrato che la risposta iperplasica del fegato in seguito al trattamento con una singola dose di TCPOBOP, evidenziata dall'aumentata incorporazione della bromodeossiuridina (BrdU) e dall'incremento della proteina *proliferating cell nuclear antigen* (PCNA), è associata ad un notevole incremento dei livelli proteici del co-attivatore YAP e dei livelli dell'mRNA del suo gene target, *baculoviral inhibitor of apoptosis repeat-containing 5* (Birc5/survivin). Al contrario, la somministrazione di una seconda dose di TCPOBOP, non causa né un'ulteriore crescita della massa epatica, né un'aumento dei livelli proteici dello YAP, suggerendo che la *Hippo pathway* è coinvolta nella refrattarietà del fegato agli ulteriori stimoli mitogenici. Negli epatocarcinomi sviluppati nei topi sottoposti al trattamento DENA + TCPOBOP è stata osservata l'overespressione e la traslocazione nucleare dello YAP. L'incremento nell'espressione dello YAP negli epatocarcinomi è risultato essere accompagnato dall'overespressione dei livelli dell'mRNA per l'*alfa-fetoprotein* (AFP) e il *connective tissue growth factor* (CTGF), riconosciuti come geni target dello YAP, e da una significativa down-regolazione del miRNA-375. Su questi basi i presenti dati suggeriscono che la *Hippo pathway* svolge un ruolo critico nella regolazione dell'accrescimento del fegato indotto da TCPOBOP, consentendoci di ipotizzare che questa cascata chinasica probabilmente non risulta più attiva nelle cellule tumorali che, pertanto, diventano resistenti all'effetto soppressivo sulla crescita, che si può osservare nel tessuto normale circostante, e si espandono clonalmente fino a formare HCCs.

Chapter 1

Introduction

1.1 - Background

How multicellular organisms orchestrate the growth of their individual cells and eventually the size of the respective organs is a primary question that has drawn the attention and interest of entire generations of biologists. In the past decade, much has been learned about tissue growth control, but it is evident that the comprehension of this process is far from complete.

The liver is an interesting organ which in adult organisms is in a quiescent state but under certain conditions shows a remarkable regenerative capacity. In fact, following a 2/3 surgical resection, most of the liver size is regained within 3 to 4 days (Higgins and Anderson, 1931). After the initial growth, no further enlargement of the liver is observed, suggesting the existence of pathways leading to termination of liver regeneration. While some studies have initially proposed transforming growth factor-beta (TGF-β) as the terminator of liver regeneration (Michalopoulos, 2007), given its mitoinhibitory properties and its upregulated expression as regeneration progresses, no clear evidence has ever been achieved. Moreover, it is unknown how the liver senses this termination signal or what the underlying mechanism/s involved is/are.

Even more striking is the capacity of the liver to modify its size in response to physiologic stimuli (such as hepatic enlargement during pregnancy) or in response to xenobiotics with mitogenic potency. Many xenobiotics able to induce liver enlargement are ligands of the nuclear receptor superfamily and interestingly are also non-genotoxic liver carcinogens (Germain *et al.*, 2006). In spite of several studies, the key molecular events which govern the tumoral potency of ligands of nuclear receptors are still unclear. The breakthrough that many compounds which possess liver tumor promoting ability are also potent inducers of hepatocyte proliferation led to the supposition that the mechanisms by which these agents cause liver neoplasia are a consequence of their mitogenic capacity that ultimately results in an increased rate of mutation (Marsman *et al.*, 1988; Ames and Gold, 1990). However, it can be hypothesised that tumors arising in these enlarged livers may be the consequence of the ‘escape’ of ‘selected’ cells from the regulatory mechanism/s governing the size of the organ.

Accumulating evidence suggests that a 'size checkpoint' operates at the level of the organ's total mass, rather than on the size or number of the constituent cells. Coordination of cell proliferation and death is essential not only to attain proper organ size during development, but also for maintaining tissue homeostasis throughout postnatal life. In *Drosophila*, these two processes are orchestrated by the Hippo kinase cascade, a growth suppressive pathway that ultimately antagonizes the transcriptional coactivator Yorkie (Yki). Components of the Hippo pathway, known to be crucial in control of organ size are highly conserved in mammals (for review, Edgar, 2006). Genetic and biochemical studies gradually structured the current model, in which the mammalian sterile-20-like kinase 1/2 (Mst1/2) interact with the WW domain-containing adapter protein (WW45) to phosphorylate and activate the large tumor suppressor kinase 1/2 (Lats1/2) (Chan *et al.*, 2005; Callus *et al.*, 2006). Lats1/2 kinase is also activated by the Mps one binder kinase activator protein (Mob1) (Praskova *et al.*, 2008). Subsequently, Lats1/2 directly phosphorylate, hence inactivate via cytoplasmic sequestration the transcriptional coactivator Yes-associated protein (YAP, mammalian homolog of Yki) (Zhao *et al.*, 2007; Hao *et al.*, 2008). Dysregulation of the Hippo pathway results in YAP dephosphorylation, thus its activation (through loss of the kinase cascade), leading to nuclear translocation where it binds to transcription factor/s and regulates the transcription of this pathway's target genes (Zhao *et al.*, 2008).

It has been reported, using conditional YAP transgenic mouse models, that YAP induces a dramatic increase in liver size and eventually leads to hepatocellular carcinoma (HCC) formation, its overexpression phenocopying the loss of the Hippo pathway components (Camargo *et al.*, 2007; Dong *et al.*, 2007), related to organ size control.

1.2 - Direct hyperplasia

In the past two decades a vast number of agents were identified to be able to directly stimulate hepatocyte proliferation in the absence of cell loss. This hepatic proliferation induced by such agents, termed direct mitogens, was denominated as direct hyperplasia (Columbano and Shinozuka, 1996). Such replicative modality leads to an increase of hepatocyte DNA synthesis resulting in a significant liver mass growth within 2-3 days. The potency of the mitogenic stimulus and the peaks of the S phase vary according to the nature of the agents (Columbano *et al.*, 2003). These direct mitogens include a broad spectrum of chemicals with little structural similarity such as peroxisome proliferators (PPs), retinoic acids (RAs), triiodothyronine (T3) and the halogenated hydrocarbon 1,4-bis[2-(3,5-dichloropyridyloxy)]benzene (TCPOBOP) (for review, Columbano and Shinozuka, 1996).

Mitogen/s	**Receptor/s**
Peroxisome Proliferators	Peroxisome Proliferator Activated Receptors
Retinoic Acids	Retinoic Acid Receptors
Triiodothyronine	Thyroid Hormone Receptors
Halogenated Hydrocarbons	Constitutive Androstane Receptor

Table 1 The main mitogens and their respective receptor/s, through which they induce direct hyperplasia.

1.2.1 - Nuclear receptor superfamily

The above mentioned mitogens are all ligands of different receptors belonging to the nuclear receptor superfamily, namely the peroxisome proliferator activated receptors (PPARs), retinoic acid receptors (RARs), thyroid hormone receptors (TRs) and constitutive androstane receptor (CAR) (Mangelsdorf *et al.*, 1995; Tzameli *et al.*, 2000). Subsequent to the activation by the respective ligands these receptors act as transcription factors. In fact, following the binding with the respective ligands, PPARs,

RARs, TRs and CAR homodimerize or heterodimerize with 9-*cis*-retinoic acid receptor (RXR), forming transcriptional active dimers which are able to bind to specific elements of the DNA, made up of an AGGTCA nucleotide sequence (Kliewer *et al.*, 1992). Once bound to the DNA, the dimers directly regulate the expression of target genes implicated in lipid metabolism, cell differentiation, cell proliferation and xenobiotic metabolism or act through cross-talking with other signal transduction pathways (Aranda and Pascual, 2001). The transcriptional activity of these nuclear receptors is regulated through the recruitment of corepressor and coactivator proteins. Corepressors constitute various multiprotein complexes which have a deacetylase activity. This deacetylation increases the density of chromatin leading to the repression of transcription. On the contrary, following ligand binding, the receptors undergo a transconformational change which allow the recruitment of coactivators. Some of these proteins are chromatin remodeling factors which hold acetylase histone activity, while others can act directly with the transcriptional machinery. Recruitment of coactivator complexes by the promoter target cause chromatin decondensation and subsequently induce transcriptional activity. The characterization of corepressors and coactivators, together with the identification of the domains through which they interact specifically with the receptor, has demonstrated the existence of a molecular mechanism by which these receptors bring about their transcriptional action on target genes (McKenna *et al.*, 1999; Xu *et al.*, 1999; Dilworth and Chambon, 2001).

1.2.1.1 - CAR

This receptor, highly expressed in the liver, is active in the absence of ligand with the unique capability to be further regulated by activators. CAR is compartmentalized in the cytoplasm in a similar manner to other nuclear receptors (Kawamoto *et al.*, 1999). Retention in the cytoplasm prevents chronic activation of its target genes and allows tight regulation of the receptor's activity. Two endogenous ligands, androstenol and androstanol (both metabolites of androstane), interact directly with CAR to repress its constitutive activity (Forman *et al.*, 1998). Activators (mainly drugs and xenobiotics) either bind directly to CAR, consistent with other family members, or act indirectly,

such as phenobarbital (PB), which do not bind to the receptor but translocate CAR to the nucleus, making translocation an initial step in the CAR activation process (Kawamoto *et al.*, 1999; Zelko *et al.*, 2001). A phosphorylation cascade is involved in regulating CAR translocation, yet elucidation of the CAR activation mechanism has proved difficult due to the fact that CAR accumulates spontaneously in the nucleus of transformed cell lines regardless of activation state (Kawamoto *et al.*, 1999). A protein capable of retaining CAR in the cytoplasm of transformed cell lines has now been identified, facilitating the elucidation of the exact activation mechanism hopefully in the near future (Kobayashi *et al.*, 2003). Moreover, it has become apparent that translocation alone does not determine CAR activation, but that additional regulation is required in the nucleus (**Fig. 1**).

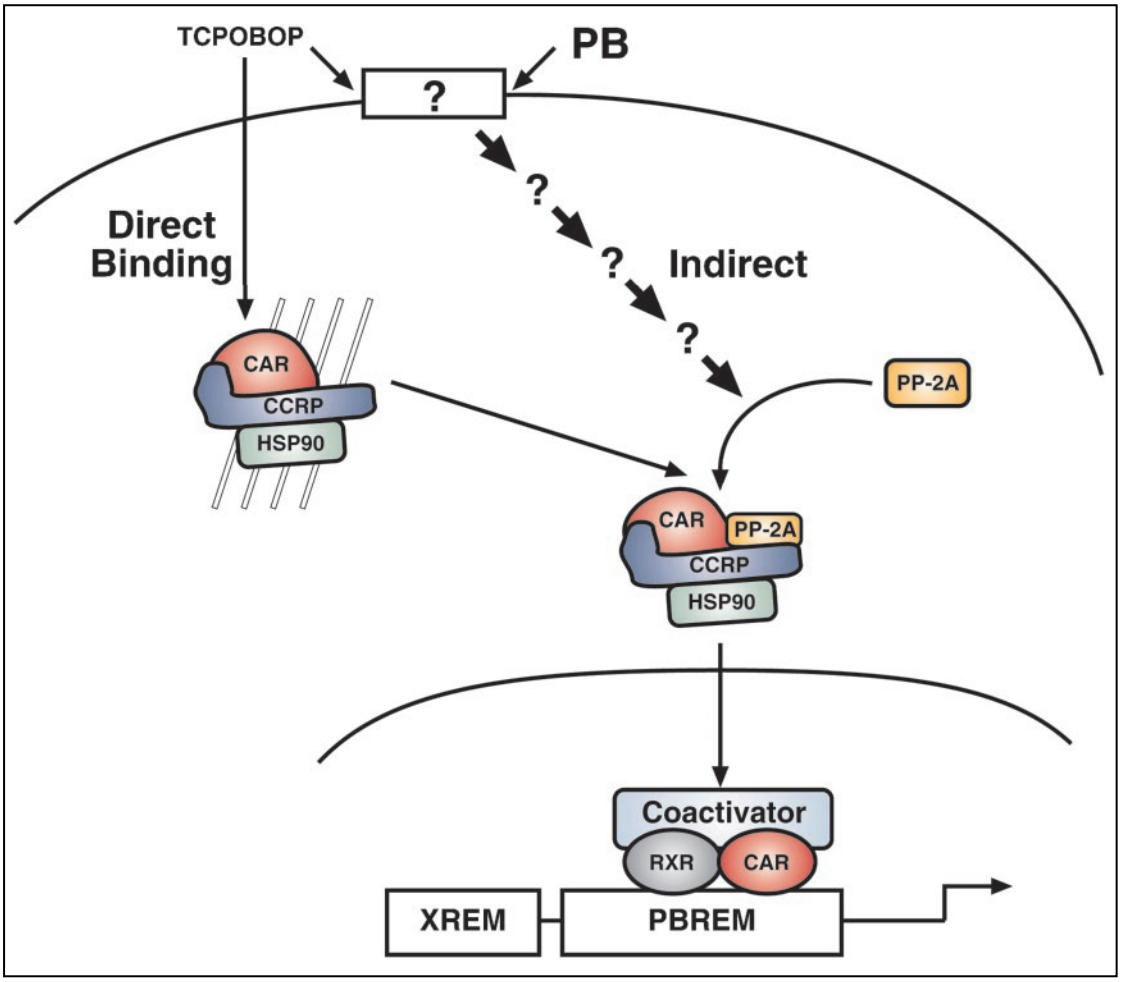

Fig. 1 CAR translocation can be induced by either direct ligand binding to the receptor, or indirectly, via a partially elucidated signal transduction pathway. CAR exists in a complex with heat shock protein 90 (Hsp90), retained in the cytoplasm by the

cochaperone cytoplasmic CAR retention protein (CCRP). Indirect activators or the direct binding of ligands to CAR subsequently recruits protein phosphatase 2A (PP2A) to the complex. Once in the nucleus, further activation steps involving calmodulin-dependent kinase and recruitment of coactivators occur before DNA binding and transcriptional activation of target genes (Swales and Negishi, 2004).

CAR has been identified as a mediator of the induction of cytochrome P450 (CYP) gene expression, especially *cytochrome P450, family 2, subfamily b, polypeptide 10* (*Cyp2b10*) in response to a particular class of xenobiotic compounds (Honkakoski *et al.*, 1998a; Honkakoski *et al.*, 1998b; Sueyoshi *et al*., 1999). These chemicals, exemplified by PB, markedly increase expression of this CYP enzyme and other proteins involved in metabolism and thus elimination of drugs and other xenobiotic compounds (Wei *et al.*, 2000; Maglich *et al.*, 2002; Ueda *et al.*, 2002; Wei *et al.*, 2002; Honkakoski *et al.*, 2003; Rosenfeld *et al.*, 2003). Although they do not share any apparent chemical similarities, these compounds are collectively referred to as 'PB-like' inducers, on the basis of their similar biological responses. The most potent of these xenobiotics, originally isolated as a pesticide contaminant (Poland *et al.*, 1980), is TCPOBOP. Even quite low concentrations of this xenobiotic agent efficiently activate CYP gene expression in mice (Poland *et al.*, 1980; Poland *et al.*, 1981; Raunio *et al.*, 1988; Kelly *et al.*, 1990; Diwan *et al.*, 1992; Smith *et al.*, 1993). Perhaps the simplest of several possible mechanisms to account for the effects of TCPOBOP is that it acts as an agonist ligand for CAR, resulting directly in Cyp2b10 gene activation. This mechanism has been strongly supported by results that are the mirror image of those obtained with the inverse agonists (Tzameli *et al.*, 2000). Thus, binding of TCPOBOP significantly increases coactivator recruitment by CAR, both *in vitro* and *in vivo*.

1.2.1.1.1 - TCPOBOP

TCPOBOP is the most potent CAR agonist, with respect to other drugs and xenobiotics (including PB), reported to induce liver hyperplasia and hypertrophy in mice (Dragani *et al.*, 1985; Manenti *et al.*, 1987). Similar to other xenobiotics, this hepatic mitogen

achieves such effect by accelerating the entry of hepatocytes into the S phase of the cell cycle (Ledda-Columbano *et al.*, 2000). A single administration of TCPOBOP is much more effective in inducing hepatocyte proliferation in females than in males (Ledda-Columbano *et al.*, 2003). Such proliferative response remains efficient during all adult life (Ledda-Columbano *et al.*, 2004). Moreover, TCPOBOP given chronically was found to be a non-genotoxic hepatocarcinogen. In addition, it is reported to be the most powerful liver tumor promoter, when compared to other drugs and xenobiotics (comprising PB), by the criterion of increased numbers of diethylnitrosamine (DENA)-initiated preneoplastic foci in mice (Dragani *et al.*, 1985; Diwan *et al.*, 1986; Romano *et al.*, 1986; Dragani *et al.*, 1987; Diwan *et al.*, 1988; Diwan *et al.*, 1992). TCPOBOP results in a high percentage of liver tumor metastases to the lung, implying effects on tumor progression. Although TCPOBOP does not cause liver tumor promotion in rats, it does increase the incidence of nasal cavity tumors in DENA-treated rats but not mice (Diwan et al., 1992).

1.3 - Hippo signaling pathway

Meticulous control of cell proliferation and death is crucial for attaining correct organ size during development but also for maintaining proper organ regeneration. Such process is an essential function of multicellular organisms under physiological conditions. Impairment of this function frequently leads to tumorigenesis (Conlon and Raff, 1999). Signaling pathways transmitting extra and intracellular signals leading ultimately to gene transcription are at the core of organ size regulation studies. Initial studies in *Drosophila* and more recent ones in mammals have demonstrated the fundamental role of the Hippo signaling pathway in controlling organ size by regulating not only cell proliferation but also apoptosis. In *Drosophila* loss of the kinase cascade components lead to massive tissue overgrowth characterized by excessive cell proliferation and diminished apoptosis suggesting the importance of the Hippo pathway in organ size control (for review, Edgar, 2006). Furthermore, it was demonstrated that the mammalian pathway is not only implicated in the regulation of organ size but more

importantly that its dysregulation leads to carcinogenesis in transgenic mouse models (Camargo *et al.*, 2007; Dong *et al.*, 2007).

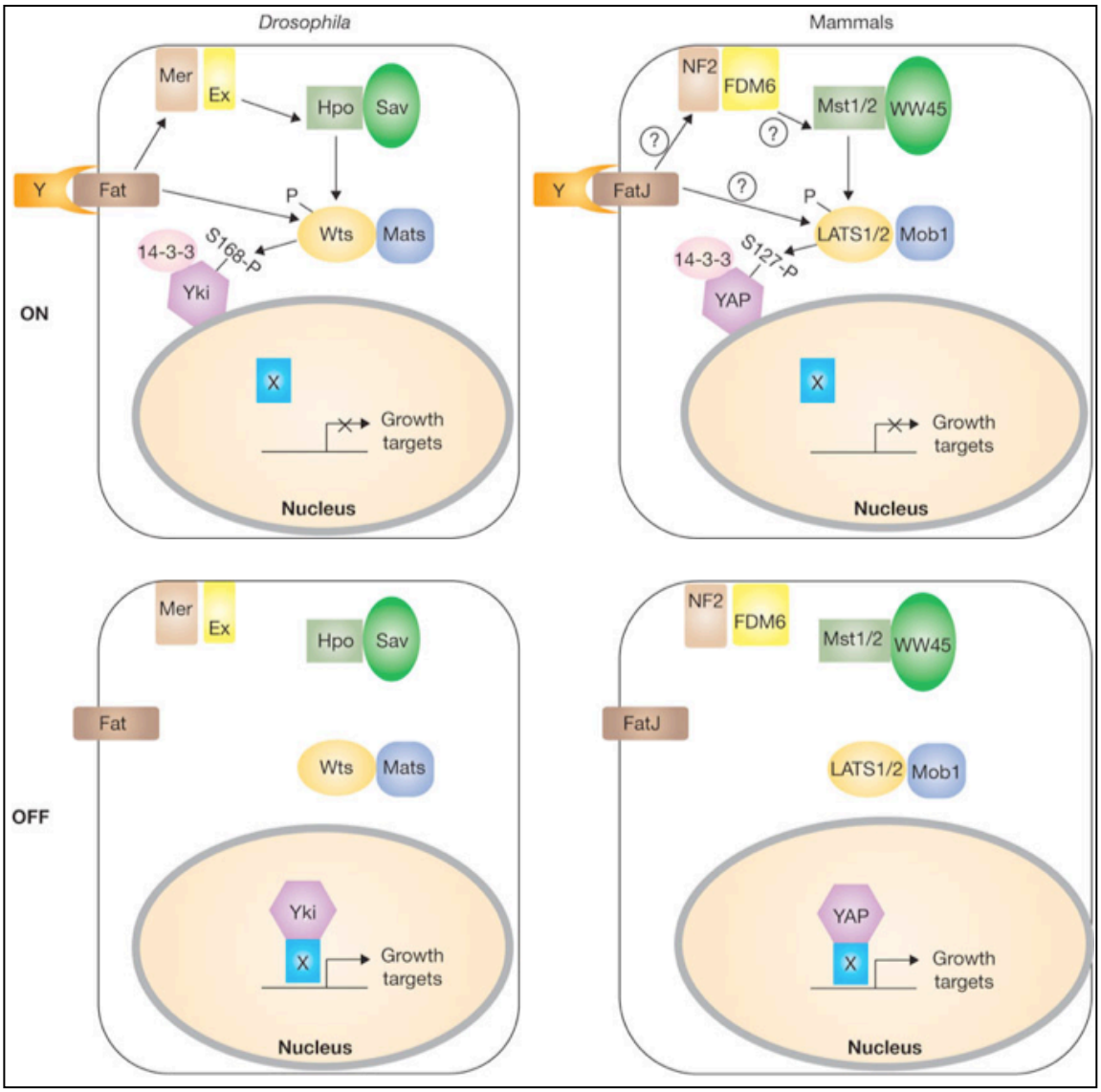

Fig. 2 The Hippo signaling pathway was initially described in *Drosopila* (left panels) and more recently confirmed in mammals (right panels). The *Drosophila*'s kinase cascade components are highly conserved in the mammalian signaling pathway (respective homologs showing the same shape and color). Hippo pathway activation (upper panels) causes phosphorylation of the downstream effector Yki/YAP by Warts (Wts)/Lats1/2, thus bringing about its inactivation via cytoplasmic sequestration. On the contrary, inactivation of Hippo pathway (lower panels) results in Yki/YAP dephosphorylation leading to nuclear translocation where it binds to transcription factors/s and subsequently induces growth target genes (Buttitta and Edgar, 2007).

1.3.1 - Drosophila

Drosophila genetic mosaic screens resulted to be a powerful tool in the elucidation of the Hippo signaling pathway. In the past decade, studies gradually structured the current model, from the core components to the downstream effectors. Recent studies showed that this kinase cascade functions as a regulator of organ size, signaling through sequential phosphorylation-mediated inactivation of the transcriptional coactivator Yki (Huang *et al.*, 2005). This function is achieved at least in part by transcriptional activation of *cyclin E*, *thread* (which encodes Drosophila inhibitor of apoptosis protein 1 (diap1)) (Wu *et al.*, 2003) and the microRNA (miRNA) *bantam* (Nolo *et al.*, 2006; Thompson and Cohen, 2006). Dysfunction of the Hippo pathway results in excessive cell proliferation and diminished apoptosis leading ultimately to massive tissue overgrowth.

1.3.1.1 - Core components

The first Hippo signaling pathway component to be identified was *Wts* which encodes a nuclear dumbbell forming-2-related (NDR) family protein kinase. *Wts* mutation lead to considerable tissue overgrowth without affecting cell fate determination (Justice *et al.*, 1995; Xu *et al.*, 1995). Subsequently, *Salvador* (*Sav*) encoding a WW domain-containing adaptor protein and *Hippo* (*Hpo*) encoding a Sterile-20 (Ste-20) family protein kinase were identified as other components of the Hippo pathway. In this complex, Hpo kinase interacts directly with the scaffold protein Sav and promotes Wts kinase phosphorylation (Pantalacci *et al.*, 2003; Udan *et al.*, 2003; Wu *et al.*, 2003). The WW domain of Sav was found to mediate its binding with Wts, while the C-terminal domain is crucial for its interaction with Hpo (Harvey *et al.*, 2003). Furthermore, *Drosophila* Ras-association domain family ortholog (dRASSF) was considered to restrict Hpo activity through competition with Sav for interaction with Hpo (Polesello *et al.*, 2006). Mutation or deletion of either *Sav* or *Hpo* leads to promotion of cell proliferation and restriction of apoptosis resulting ultimately in similar effects to that of *Wts* (Kango-Singh *et al.*, 2002; Tapon *et al.*, 2002; Harvey *et al.*, 2003; Jia *et al.*, 2003).

Later on, *Mats* which encodes a Mob1-related protein was identified as the last core component of this kinase cascade. The Mats protein interacts physically with Wts as an activating subunit. Moreover, Mats is also phosphorylated by Hpo, enhancing the kinase activity of Wts in this complex. *Mats* mutation, like alterations of the previous components, lead to significant organ overgrowth through the promotion of cell proliferation and restriction of apoptosis (Lai *et al.*, 2005; Wei *et al.*, 2007; Shimizu *et al.*, 2008).

These studies converge on the main role of the *Drosophila* Hippo signaling pathway, that of restricting cell proliferation and promoting apoptosis. This function is achieved at least in part by transcriptional regulation of *cyclin E*, *diap1* (Wu *et al.*, 2003) and the miRNA *bantam* (Nolo *et al.*, 2006; Thompson and Cohen, 2006).

1.3.1.2 - Downstream effectors

The protein levels of cyclin E and Diap1 were found to be controlled at the transcriptional level rather than a consequence of post translational modification of the proteins (Wu *et al.*, 2003). This meant that there should be a downstream effector that could carry on the message of the core components of this kinase cascade to the machinery that regulates the transcription of the respective genes. The missing link was identified to be the transcriptional coactivator Yki, using protein interaction screening with Wts kinase (Huang *et al.*, 2005). A biochemical study showed that Wts protein kinase directly phosphorylates Yki, amongst other (two) sites, at the crucial serine (S) 168 residue. Phosphorylation at S168 induces Yki binding to the 14-3-3 protein, leading to its cytoplasmic retention and inactivation. Mutation of Yki S168 lead to the constitutive activation and nuclear translocation of Yki which subsequently induces the transcription of the Hippo pathway target genes resulting ultimately in enhanced cell proliferation and reduced apoptosis, hence tissue overgrowth (Dong *et al.*, 2007, Zhang *et al.*, 2008b).

Since the transcription coactivator Yki possesses no DNA-binding activity, the next step was to identify target transcription factors that bring about Yki activity. Yki yeast two-hybrid data led to the identification of *Scalloped* (*Sd*), encoding a transcriptional enhancer activator DNA (TEAD)-binding domain, as Yki associated transcriptional factor mediating Yki-induced gene expression and overgrowth phenotype (Goulev *et al.*, 2008). In fact, Sd was also found to nuclearly localize and recruit Yki to the promoter region of the pathway-responsive gene diap1, further confirming the latter as a direct transcription gene of the Hippo signaling pathway (Zhang *et al.*, 2008b). Mutation of *Sd* abrogated proliferation and survival of wing imaginal disc cells (Wu *et al.*, 2008; Zhang *et al.*, 2008b; Zhao *et al.*, 2008). Affinity chromatography and mass spectrometry applications led to the identification of Expanded (Ex), another Yki associated protein. Ex binds to Yki via WW-domain-PPxY interactions, relocalizing Yki from the nucleus to the cytoplasm, thus withdrawing its transcriptional regulatory activity (Badouel *et al.*, 2009).

1.3.2 - Mammals

Hippo signaling pathway components are well conserved from *Drosophila* to mammals. More strikingly, the mammalian kinase cascade counterparts can substitute the function of their mutant homologs in *Drosophila*, suggesting a functional conservation of these components (for review, Edgar, 2006). Recent studies confirmed that the mammalian Hippo pathway also functions as a regulator of organ size, signaling through the same mechanism of action, leading to phosphorylation, thus inactivation of the transcriptional coactivator YAP (Dong *et al.*, 2007). Such function is attained by transcriptional activation of target genes such as *baculoviral inhibitor of apoptosis repeat-containing 5* (*Birc5*) (Dong *et al.*, 2007), *connective tissue growth factor* (*CTGF*) (Zhao *et al.*, 2007) and *alpha-fetoprotein* (*AFP*) (Dong *et al.*, 2007). Dysfunction of the Hippo pathway results not only in remarkable cell proliferation and restricted apoptosis, leading to immense tissue overgrowth but also in oncogenesis.

1.3.2.1 - Core components

The highly conserved core components of the Hippo signaling pathway from *Drosophila* to mammals have been identified as Mst1/2 (Hpo homolog), WW45 (Sav homolog), Lats1/2 (Wts homolog) and Mob1 (Mats homolog). In this complex, Mst1/2 play an essential role in regulating the other three components.

Mst1/2 encoding a Ste-20 family protein kinase were identified as the first components of the mammalian Hippo pathway. In this kinase cascade, Mst1/2 kinases assemble the core components and promote Lats1/2 kinases phosphorylation (Chan *et al.*, 2005). Besides these central roles, Mst1/2 have been shown to interact with other components external to this pathway, mainly involved in apoptosis. Mst1/2 are associated with RASSF members (Khokhlatchev *et al.*, 2002); RASSF1A is physically associated with Mst1. Initially, it was demonstrated that RASSF1A inhibits Mst1 kinase activity (Praskova *et al.*, 2004). However, a more recent study has shown that overexpression of RASSF1A promotes Fas-induced apoptosis via Mst1 activation (Oh *et al.*, 2006). In addition, RASSF2 was found to be associated with Mst2. RASSF2 stabilizes Mst2 from degradation, while its deletion decreases the levels of Mst2 leading to inhibition of apoptosis (Cooper *et al.*, 2009). The role of Mst2 in apoptosis was reported to be inhibited by the binding of Raf-1, forming an Mst2 complex which hinders its phosphorylation (O'Neill *et al.*, 2004). However, stress signals can dissociate such complex resulting in Mst2 phosphorylation and ultimately apoptosis (O'Neill and Kolch, 2005). Deletion of *Mst1/2* in liver led to YAP phosphorylation inability, sufficient to initiate hepatocyte proliferation and resistance to apoptosis, resulting in dramatic liver growth and development of HCC (Zhou *et al.*, 2009; Lu *et al.*, 2010; Song *et al.*, 2010). In spite of that, the effect of Mst1/2 deficiency on organ size is more substantial in certain organs (e.g. liver and stomach), than in others (e.g. kidney), which do not manifest such repercussions at all (Song *et al.*, 2010). This is due to the probable difference, from one organ to another, in the contribution of impaired cell differentiation versus cell number on the overall size of the organ. Likewise, the role of Mst1/2 in this pathway is presumably to be cell context-dependent, since Mst1/2 are not necessary for Lats1/2 phosphorylation and for cell density-induced YAP nuclear-cytoplasmic

translocation in mouse embryonic fibroblast (MEF) cells, or YAP phosphorylation in early embryos (Zhou *et al.*, 2009; Oh *et al.*, 2009).

Subsequently, *WW45* encoding a WW domain-containing adaptor protein was identified as another component of the mammalian Hippo signaling pathway. WW45 interacts physically with Mst1/2 through the Sav/RASSF/Hpo (SARAH) domain present in both proteins. WW45 can also be directly phosphorylated and stabilized by Mst1/2 (Chan *et al.*, 2005; Callus *et al.*, 2006). Recent studies, have shown that WW45 is required for Mst1 activation. Homozygous loss of *WW45* resulted to be embryonic-lethal, with various organs exhibiting hyperplasia and immature differentiation in epithelium, while heterozygous deletion led to higher susceptibility to tumorigenesis (Lee *et al.*, 2008). Moreover, it was demonstrated that suppression of WW45 hinders the already described Mst1-mediated apoptosis (Luo *et al.*, 2009). In addition, conditional ablation of *WW45* in the liver resulted not only in organ size enlargement but also led to tumor formation. Despite that, unexpectedly, phosphorylation of Lats1/2 and YAP were not affected, suggesting that WW45 is not absolutely required for the activation of Lats1/2 and can regulate tissue growth in the liver by some other mechanism/s (Lu *et al.*, 2010).

Lats1/2 encoding a NDR family protein kinase were identified as further components of the mammalian Hippo pathway. Lats1/2 are phosphorylated at the hydrophobic motif by Mst1/2, followed by the subsequent autophosphorylation of their activation loop (Chan *et al.*, 2005). Deletion of *Lats1* in mice resulted in higher liability to soft tissue sarcoma and ovarian tumor development (St John *et al.*, 1999), while deficiency of *Lats2* demonstrated to be embryonic-lethal (McPherson *et al.*, 2004; Yabuta *et al.*, 2007). Similarly, downregulation of Lats1 was found in human soft tissue sarcoma (Hisaoka *et al.*, 2002), astrocytoma (Jiang *et al.*, 2006) and breast cancer (Morinaga *et al.*, 2000; Takahashi *et al.*, 2005). Last1/2 are able to phosphorylate, thus inactivate YAP *in vitro* and in cell culture (Zhao *et al.*, 2007; Hao *et al.*, 2008). Nonetheless, it has been reported that the role of Lats1/2 in YAP phosphorylation is dependent on the cell type. In MCF10A cells, overexpression of Lats1 solely was found to inhibit YAP-induced epithelial-to-mesenchymal transition (EMT), cell migration and anchorage-independent growth (Zhang *et al.*, 2008a). However, deletion of both Lats1 and 2 was shown to be

required for an efficient inhibition of YAP phosphorylation in HeLa cells. Recent studies in the liver, have demonstrated contentious results regarding the necessity of Mst1/2 for Lats1/2 phosphorylation, even though there was a reduction in YAP phosphorylation (Zhou *et al.*, 2009; Lu *et al.*, 2010). In fact, fractionation experiments suggested the possibility of YAP phosphorylation by a Mst1/2-regulated kinase different from Lat1/2 (Zhou *et al.*, 2009). Nevertheless, the chance that the other NDR family members may phosphorylate YAP was diminished by the fact that *in vitro* there is no NDR1/2-YAP interaction and in cell culture NDR1/2 overexpression does not induce YAP phosphorylation (Hao *et al.*, 2008). Hence, Lats1/2 remain the main kinases that bring about YAP phosphorylation, yet the involvement of other kinases cannot be excluded.

Later on, Mob1 was identified as the last core component of the mammalian kinase cascade. Mob1 is phosphorylated by Mst1/2, which enhances the interaction between Mob1 and Lats1/2, eventually promoting the phosphorylation of Lats1/2 (Yabuta *et al.*, 2007; Hirabayashi *et al.*, 2008; Praskova *et al.*, 2008; Chow *et al.*, 2010). Notwithstanding, the exact mechanism of how Mob1 induces the activation of Lats1/2 is not well comprehended. Initial studies, have established that Mob1 artificial targeting to plasma membrane bring about Lats1 membrane localization and the subsequent activation (Hergovich *et al.*, 2006). Accordingly, Mats (Mob1 homolog in *Drosophila*) was shown to localize to plasma membrane, and this membrane-localized form, contrary to the wild-type protein, inhibits tissue overgrowth when overexpressed (Ho *et al.*, 2009). In spite of that, endogenous Mob1 membrane localization has not been substantiated. Besides, the mechanism of how Mob1/Mats membrane localization is brought about is still not clear. A recent study *in vitro*, demonstrated that Mob1 in the presence of Mst3 activates NDR2 without having an effect on its hydrophobic motif phosphorylation, suggesting another mean of NDR activation by Mob1 which could possibly apply to Lats1/2 activation too (Stegert *et al.*, 2005).

1.3.2.2 - Downstream effectors

Components of the Hippo signaling pathway so far proved to be highly conserved from *Drosophila* to mammals. This was further confirmed by the identification of the transcriptional coactivator YAP and its paralog transcriptional co-activator with PDZ binding motif (TAZ) (both Yki homologs) acting as the major downstream effectors of the mammalian Hippo pathway. *YAP* was first reported to be located on chromosome 11q13 (Sudol *et al.*, 1995) but later the 11q22 chromosome was also associated to this gene (Overholtzer *et al.*, 2006; Zender *et al.*, 2006). YAP has an N-terminal proline-rich domain, a TEAD-binding region, two WW domains (or one in the YAP1 splicing variant) (Sudol *et al.*, 1995; Komuro *et al.*, 2003), an SH3-binding motif, a coiled-coil domain, a transcription activation domain, and a C-terminal PDZ-binding motif. *TAZ* was found to be located on chromosome 3q24 (Kanai *et al.*, 2000). TAZ has a similar domain organization to YAP, although it lacks the proline-rich domain, the second WW domain, and the SH3-binding motif.

YAP functionality was later demonstrated to depend on the presence of an intact WW domain/s (Yagi *et al.*, 1999; Komuro *et al.*, 2003).

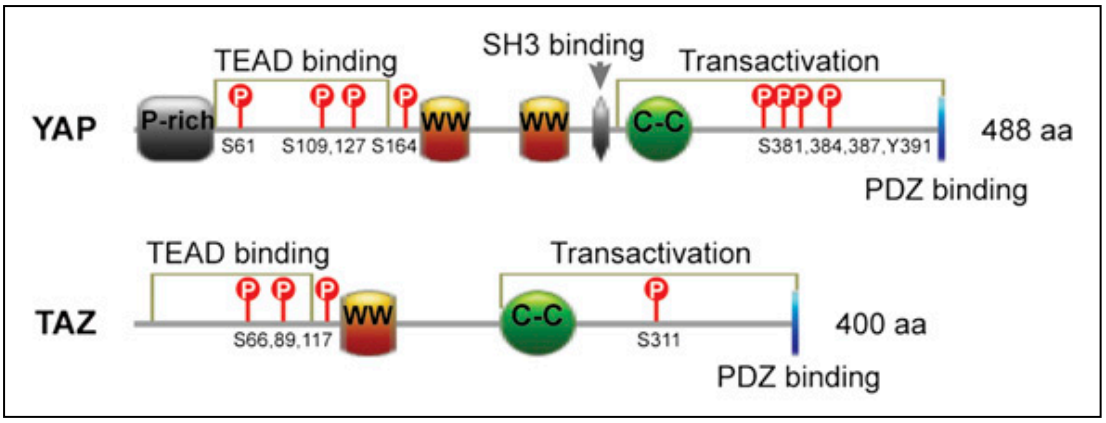

Fig. 3 Domain organization of YAP and TAZ proteins (Zhao *et al.*, 2010). WW domain (WW); proline-rich domain (P-rich); coiled-coil domain (C-C). YAP/TAZ is phosphorylated by Lats1/2 on S61, S109, S127, S164 and S381/S66, S89, S117, S311 in the HXRXXS motifs. S127/S89 phosphorylation induces 14-3-3 binding, resulting in cytoplasmic retention of YAP/TAZ (Basu *et al.*, 2003; Zhao *et al.*, 2007; Hao *et al.*, 2008; Lei *et al.*, 2008).

In fact, YAP interacts physically with Lats1/2 through the WW domain and is directly phosphorylated by the same Lats1/2 on five HXRXXS motifs (Zhao *et al.*, 2007; Hao *et al.*, 2008). These consensus motifs are also present in TAZ. As a matter of fact, TAZ is phosphorylated by Lats1/2 on similar HXRXXS motifs (Lei *et al.*, 2008). Furthermore, three of these sites are conserved and phosphorylated in Yki by Wts (Lats1/2 homolog in *Drosophila*) (Oh and Irvine, 2009). Phosphorylation of YAP S127 and the corresponding site in TAZ (S89), comparable to Yki S168 phosphorylation, resulted to be crucial for the induction of the 14-3-3 protein binding, leading to YAP/TAZ/Yki cytoplasmic retention, hence their spatial separation from nuclear target transcription factors and gene promoters (Basu *et al.*, 2003; Zhao *et al.*, 2007; Hao *et al.*, 2008; Lei *et al.*, 2008; Oh and Irvine, 2008; Ren *et al.*, 2009).

YAP/TAZ were found to inherit the conserved functions of Yki. Overexpression of YAP/TAZ can stimulate cell proliferation and suppress apoptosis by overcoming cell contact inhibition in cell culture. Moreover, YAP/TAZ can induce cell malignant transformation and promote EMT (associated with metastasis) *in vitro* (Overholtzer *et al.*, 2006; Zhao *et al.*, 2007, Camargo *et al.*, 2007; Lei *et al.*, 2008). In addition, YAP overexpression causes a dramatic increase in liver size and ultimately leads to tumor growth (Camargo *et al.*, 2007; Dong *et al.*, 2007). *In vitro* and *in vivo* experiments demonstrated that these functions of YAP/TAZ are tightly controlled by phosphorylation at the S127 and S381/S89 sites (Zhao *et al.*, 2009; Chan *et al.*, 2009). Mst1/2 and Lats1/2 were shown to inhibit YAP-mediated phenotypic changes through phosphorylation of the Hippo-responsive S sites of YAP. Mutation of these key Ss can rescue YAP/TAZ from phosphorylation, thus inactivation by Mst1/2 and Lats1/2 (Camargo *et al.*, 2007; Zhao *et al.*, 2007; Hao *et al.*, 2008; Lei *et al.*, 2008).

Lacking a DNA-binding domain, the transcriptional coactivators YAP/TAZ have to be brought to gene promoters by target transcription factors. Recent studies have established the TEAD protein family (composed of four members) as the key transcription factor target of YAP/TAZ which mediates their functions (Zhao *et al.*, 2008; Zhang *et al.*, 2009; Chan *et al.*, 2009). Hence, in conformity to the *Drosophila* homolog Sd in bringing about the biological activity of Yki (Goulev *et al.*, 2008; Wu *et*

al., 2008; Zhang *et al.*, 2008b). It has been reported in mammalian cells, that as much as 75% of TEAD2 interacts with YAP (Vassilev *et al.*, 2001). Moreover, a yeast two-hybrid screen of a human transcription factor pool also identified TEADs as the targets that are most potently activated by YAP (Zhao *et al.*, 2008). The interaction between TEAD and YAP was initially found to require TEAD C-terminal domain for YAP binding and the N-terminal of YAP as the corresponding TEAD binding domain (Vassilev *et al.*, 2001). Only recent studies have solved the three-dimensional structure of mouse and human TEAD-YAP complex, providing important insights into the molecular basis of this interaction. The C-terminal domain of TEAD forms a globular structure with a β-sandwich fold surrounded by four α-helices on one side, while the N-terminal domain of YAP wraps around TEAD, forming extensive interactions (Chen *et al.*, 2010; Li *et al.*, 2010). Deletion of *TEADs* or mutation of *TEAD Y406/YAP S94* (leading to disruption of TEAD-YAP/TAZ interaction) hinders the nuclear localization of YAP/TAZ and fades the regulation of the majority of YAP/TAZ-dependent genes, contributing to a highly diminished activity of YAP/TAZ in promoting cell proliferation, oncogenic transformation, and EMT (Lei *et al.*, 2008; Zhao *et al.*, 2008; Zhao *et al.*, 2009; Chan *et al.*, 2009; Zhang *et al.*, 2009). Additionally, deletion of both *TEAD1* and *2* demonstrated the same results obtained with YAP deletion, that of decreased cell proliferation and increased apoptosis (Sawada *et al.*, 2008).

Various gene promoters were identified to be targeted by YAP/TAZ, mediating their transcriptional activity. *Cyclin E*, like in *Drosophila,* was found to be induced by YAP *in vitro* (Zender *et al.*, 2006), although *in vivo* studies did not report a significant upregulation (Dong *et al.*, 2007). Similarly to what was observed in *Drosophila*, induction of *Birc2/cIAP1* and to a higher extent *Birc5/survivin* (*Diap1* homologs) by YAP was reported in mammals. These genes were shown to encode negative regulatory proteins that prevent apoptotic cell death (Dong *et al.*, 2007; Hao *et al.*, 2008). *Bantam*, which encodes a miRNA in *Drosophila*, is not conserved in the mammalian genome, and a functional counterpart has not been identified yet. However, other proteins including many cytokines such as CTGF and the plasma protein AFP are upregulated by YAP/TAZ in mammals (Zhao *et al.*, 2007; Dong *et al.*, 2007; Zhao *et al.*, 2008; Zhou *et al.*, 2009). In fact, CTGF was demonstrated to be a direct target gene induced by

TEAD-YAP/TAZ complex, mediating cell proliferation, adhesion, and migration (Zhao *et al.*, 2008; Zhang *et al.*, 2009). Moreover, AFP was identified as a candidate gene of YAP associated with hepatocyte proliferation (Dong *et al.*, 2007).

Drosophila	**Mammalian Homolog/s**	**Encoding Protein**	**Role in Hippo Signaling Pathway**
Hpo	Mst1/2	Ste-20 family protein kinase	Bind Sav/WW45 and Mats/Mob1 and phosphorylate Mats/ Mob1 and Wts/ Lats1/2
Sav	WW45	WW domain adaptor protein	Binds Hpo/Mst1/2, the complex binds and phosphorylates Wts/Lats1/2
Wts	Lats1/2	NDR family protein kinase	Binds Mats/Mob1 and phosphorylates Yki/YAP/TAZ
Mats	Mob1	Mob1-related protein	Binds Hpo/Mst1/2 and Wts/Lats1/2, complex enhances activity of Wts/ Lats1/2
Yki	YAP/TAZ	Transcriptional coactivator	Phosphorylated form binds 14-3-3 protein, leads to cytoplasmic retention and its inactivation. Unphosphorylated form binds Sd/ TEAD, leads to its activation and translocates to the nucleus.
Sd	TEAD	Transcription factor	Binds Yki/YAP/TAZ to regulate its target gene transcription

Table 2 Genes involved in the *Drosophila* and mammalian Hippo signaling pathway.

Chapter 2

Aim of Study

The CAR ligand TCPOBOP was previously reported to induce hepatocyte proliferation after a single dose resulting in efficient hepatomegaly in mice. However, no evidence has been provided about its effect on liver proliferation response following repeated administration. Thus the first aim of this study was:

- *to establish whether hepatocytes proliferate every time they are exposed to the mitogen TCPOBOP or if a size-control mechanism exists that prevents further growth of the liver mass in mice.*

Recent studies identified the Hippo pathway as a regulator of organ size (comprising the liver) mediating its function through the control of cell proliferation and apoptosis in genetically modified mouse models. So the objective of this research was furthered:

- *to investigate whether the Hippo pathway is eventually involved in the control of liver size following further challenge with this mitogen in mice.*

Moreover, it was formerly shown that TCPOBOP other than being able to induce hepatomegaly after a single dose, can also act as a non-genotoxic liver carcinogen following chronic administration in mice. Hence another aim of this study was:

- *to analyze the tumor incidence at various time points in a mouse carcinogenesis model, whereby tumors are initiated with a single dose of DENA and promoted by chronic exposure to the CAR agonist, TCPOBOP.*

Lately, it was demonstrated that the Hippo pathway is not only implicated in the regulation of organ size but also that its dysregulation leads to carcinogenesis (including HCC) in transgenic mouse models. Therefore the final objective of this research was:

- *to determine the subsequent role of the Hippo pathway in the DENA + TCPOBOP-induced HCC in mice.*

Current reports have suggested that the Hippo pathway networks with other well-established pathways, including the Wnt pathway in genetically modified mouse models. If an involvement of the Hippo pathway in the DENA + TCPOBOP-induced HCC will be observed, to further elucidate this correlation between the Hippo and Wnt pathway, we will analyze such pathway cooperation in these liver cancer cells.

Chapter 3

Materials and Methods

3.1 - Animals

Eight-week old female C3H/HeNCrl mice were purchased from Charles River (Milan, Italy). On arrival, the animals were given a rodent standard diet (Standard Diet 4RF21, Mucedola, Milan, Italy) and water *ad libitum* with alternating 12 hour dark/light cycles and acclimatized to laboratory conditions for 1 week before the start of the experiment. Temperature and humidity were controlled for the entire period of experimentation. Animals were maintained in accordance with the Universities Federation for Animal Welfare Handbook on the Care and Management of Laboratory Animals, and the Guidelines of the Animal Ethics Committee of the University of Cagliari. After acclimatization, the mice were randomized into four experimental protocols. Five to eight mice per experimental group were used.

3.2 - Experimental protocols

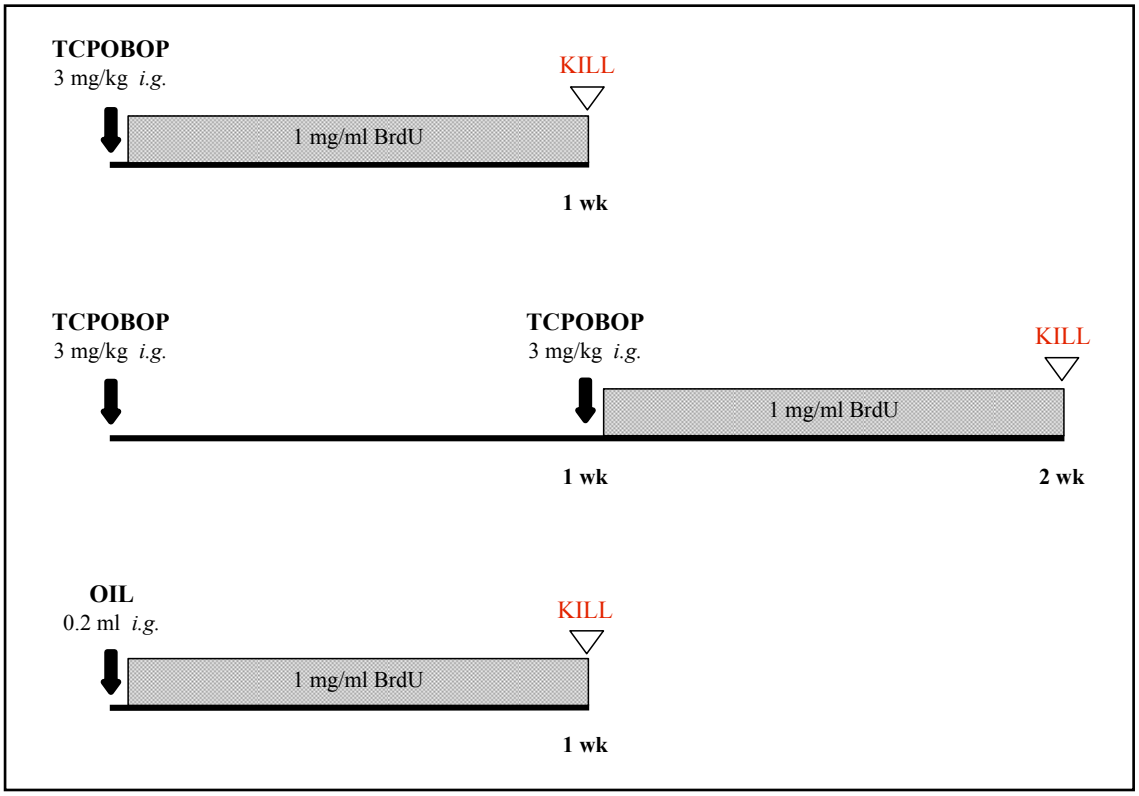

Fig. 4 Schematic representation of Experimental Protocol I

In **Experimental Protocol I**, two groups of mice were given 3 mg/kg body weight of the mitogen TCPOBOP (Cat. No. T1443, Sigma-Aldrich, St. Louis, MO, USA) dissolved in dimethyl sulfoxide (DMSO)-corn oil solution (Cat. No. D8418, Sigma-Aldrich, St. Louis, MO, USA), intragastrically. A group was sacrificed after 1 week. The remaining group was treated with another dose of TCPOBOP a week after the first dose and sacrificed 1 week after the last dose. The control group received an equivalent volume of the solvent. For determination of hepatocyte proliferation, all groups received 5-bromo-2'-deoxyuridine (BrdU) (Cat. No. B5002, Sigma-Aldrich, St. Louis, MO, USA) in drinking water [1 mg/ml] for 1 week before being sacrificed.

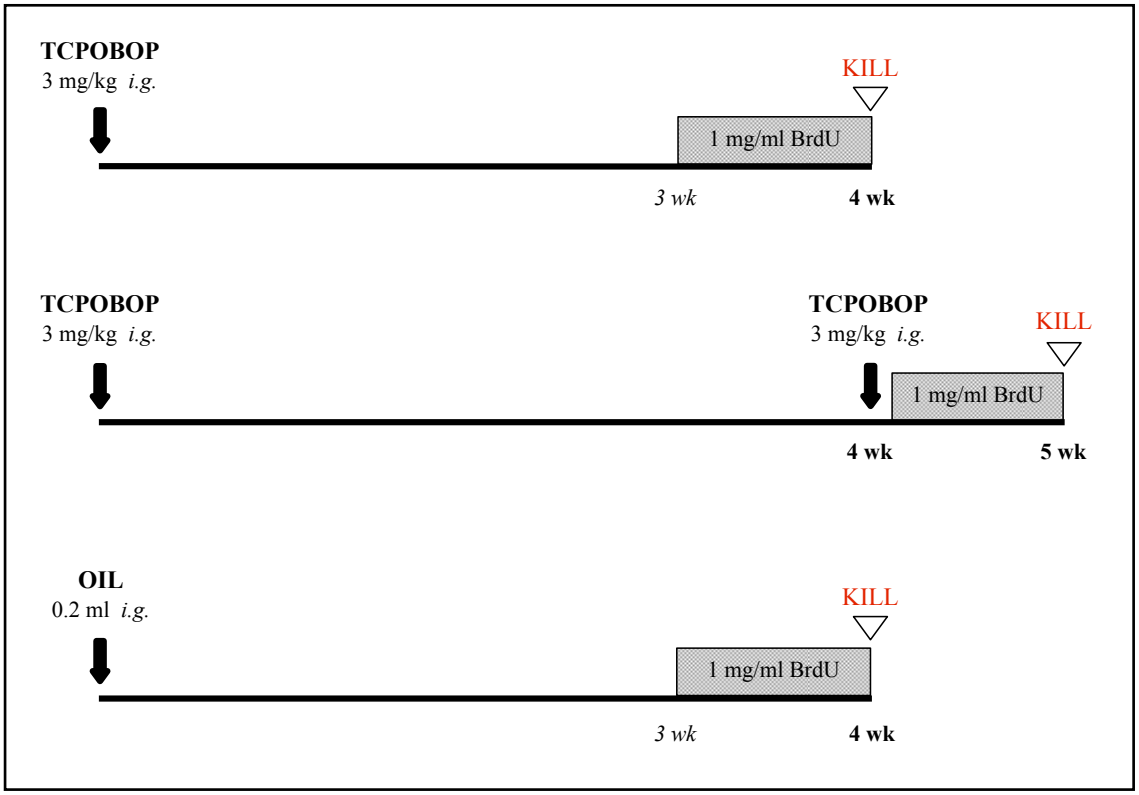

Fig. 5 Schematic representation of Experimental Protocol II

In **Experimental Protocol II**, two groups of mice were given intragastrically 3 mg/kg body weight of TCPOBOP. A group was sacrificed 1 month later. The remaining group was administered a further dose of TCPOBOP a month after the initial dose and sacrificed 1 week after the ultimate dose. The control group received an equivalent volume of the solvent. All mice received BrdU in drinking water for 1 week before being sacrificed.

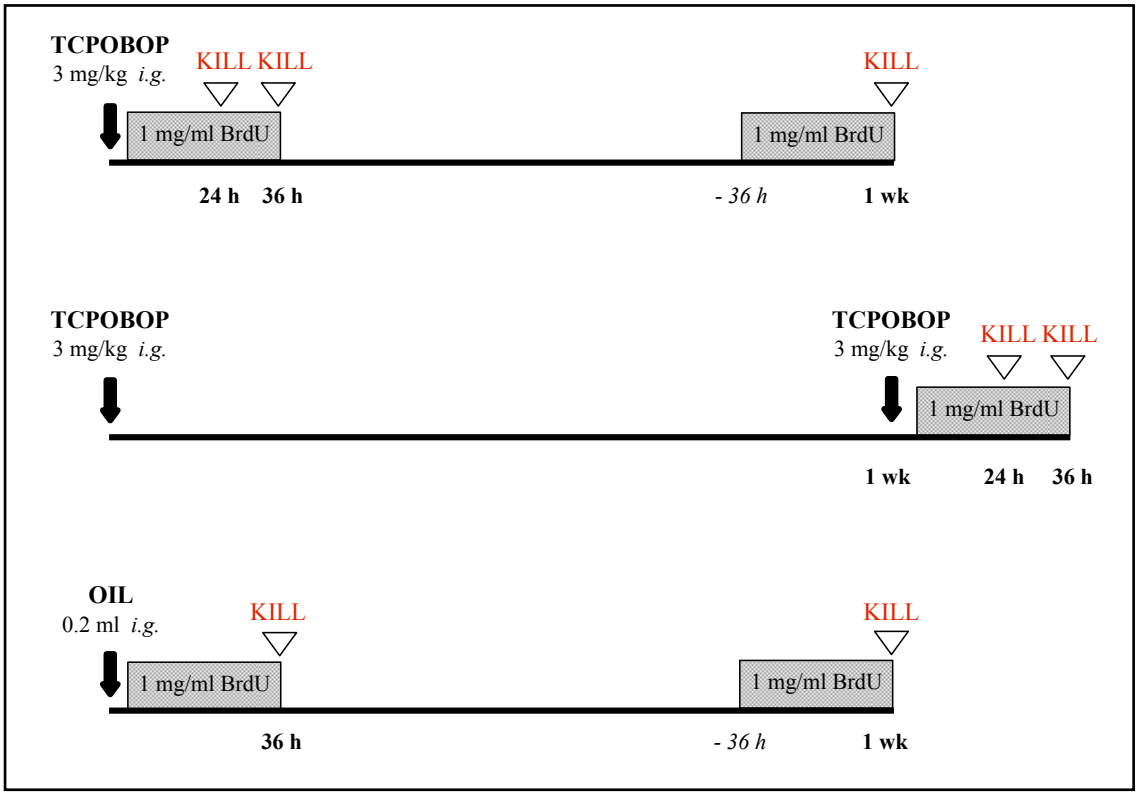

Fig. 6 Schematic representation of Experimental Protocol III

In **Experimental Protocol III**, five groups of mice were administered 3 mg/kg body weight of TCPOBOP, intragastrically. Subsequently, three groups were sacrificed 24, 36 hours and 7 days later. The other groups were given another dose of TCPOBOP, a week after the initial dose, and sacrificed 24 and 36 hours after the final dose. The respective controls received an equivalent volume of the solvent. Mice received BrdU in drinking water for 24 or 36 hours, depending on the experimental group, before being sacrificed.

Fig. 7 Schematic representation of Experimental Protocol IV

In **Experimental Protocol IV,** mice were divided into three groups. The first group was given a single intraperitoneal injection of DENA (Cat. No. N0756, Sigma-Aldrich, St. Louis, MO, USA), dissolved in saline, at a dose of 90 mg/kg body weight followed by weekly doses of TCPOBOP (3 mg/kg body weight) given intragastrically. The second group received a single intraperitoneal injection of DENA (90 mg/kg body weight) followed by weekly intragastric administrations of corn oil. The last group was only given weekly intragastric doses of TCPOBOP (3 mg/kg body weight). Mice from the three respective groups were sacrificed at three time periods: after 10, 20 and 28 weeks. All mice received BrdU in drinking water for 3 days before being sacrificed.

In all protocols, immediately after mice were sacrificed, liver sections were fixed in 10% buffer formalin and processed for staining with hematoxylin-eosin (H&E) for routine morphology or immunohistochemistry. The remaining liver was snap-frozen in liquid nitrogen and kept at -80°C until use.

3.3 - Immunohistochemistry

3.3.1 - BrdU staining

Four-micrometer-thick sections were deparaffinized, treated with 2 N HCl for 1 hour, then immersed in 0.1% Trypsin Type II-S from Porcine Pancreas (Cat. No. T7409, Sigma-Aldrich, St. Louis, MO, USA) for 30 minutes at 37°C, and incubated sequentially with 1:10 Goat Serum (Normal) (Cat. No. X0907, Dako Denmark A/S, Glostrup, Denmark) for 30 minutes, 1:50 Mouse Monoclonal Anti-BrdU Antibody (Cat. No. 347580, Becton Dickinson, San Jose, CA, USA) for 1 hour and 30 minutes, and with Dako EnVision+® System Labelled Polymer-HRP Anti-Mouse (Cat. No. K4001, DakoCytomation, Carpinteria, CA, USA) for 30 minutes. The sites of peroxidase binding were detected by 3,3'-diaminobenzidine tetrahydrochloride hydrate (DAB) (Cat. No. 261890, Sigma-Aldrich, St. Louis, MO, USA). Counter staining was performed with Harris Hematoxylin Solution (Cat. No. HHS32, Sigma-Aldrich, St. Louis, MO, USA). A segment of the duodenum, an organ with a high rate of cell proliferation, was included from each mouse to confirm delivery of the DNA precursor.

Labelling index was expressed as number of BrdU-positive hepatocyte nuclei per 100 nuclei. At least 2500 hepatocyte nuclei for each liver were scored.

3.3.2 - YAP staining

Four-micrometer-thick sections were deparaffinized, immersed in EnVision™ FLEX Target Retrieval Solution, High pH (50X) (Cat. No. DM828, Dako Denmark A/S, Glostrup, Denmark) that had been preheated to 95°C in a water bath and then heat-treated at 95°C for 40 minutes, and incubated sequentially with EnVision™ FLEX Peroxidase-Blocking Reagent (Cat. No. SM801, Dako Denmark A/S, Glostrup, Denmark) for 5 minutes, 1:100 Rabbit Polyclonal Anti-YAP (H-125) Antibody (Cat. No. sc-15407, Santa Cruz Biotechnology, Santa Cruz, CA, USA) for 1 hour and with EnVision™ FLEX/HRP Detection Reagent (Cat. No. SM802, Dako Denmark A/S, Glostrup, Denmark) for 30 minutes. The sites of peroxidase binding were detected by the mixture of EnVision™ FLEX DAB+ Chromogen (Cat. No. DM827, Dako Denmark A/S, Glostrup, Denmark), a concentrated DAB solution, and EnVision™ FLEX

Substrate Buffer (Cat. No. SM803, Dako Denmark A/S, Glostrup, Denmark) containing hydrogen peroxide. Counter staining was performed with Harris Hematoxylin Solution.

3.3.3 - Glutamine synthetase (GS) staining

Five-micrometer-thick sections were deparaffinized and incubated sequentially with 1:30 Goat Serum (Normal) for 5 minutes, 1:1000 Rabbit Polyclonal Anti-GS Antibody overnight at 4°C (Cat. No. G2781, Sigma-Aldrich, St. Louis, MO, USA), again with 1:30 Goat Serum (Normal) for 5 minutes, and with Dako EnVision+® System Labelled Polymer-HRP Anti-Rabbit (Cat. No. K4003, DakoCytomation, Carpinteria, CA, USA) for 30 minutes. The sites of peroxidase binding were detected by DAB. Counter staining was performed with Mayer's Hematoxylin Solution (Cat. No. 05-M06002, Bio-Optica, Milan, Italy).

3.3.4 - Cyp2e1 staining

Ten-micrometer-thick cryostat sections were fixed and incubated sequentially with 1:30 Goat Serum (Normal) for 5 minutes, 1:1000 Rabbit Polyclonal Anti-Cyp2e1 Antibody overnight at 4°C (Cat. No. MFO-100, Stressgen Biotechnologies Corporation, Victoria, BC, Canada), again with 1:30 Goat Serum (Normal) for 5 minutes, and with 1:20 Dako EnVision+® System Labelled Polymer-HRP Anti-Rabbit for 60 minutes. The sites of peroxidase binding were detected by DAB. Counter staining was performed with Mayer's Hematoxylin Solution.

3.4 - Western blot

Total cell extracts were prepared from frozen livers powdered in liquid nitrogen-cold mortar. Equal amounts of powder (≈50 mg) from different animals were resuspended in 1 ml Triton lysis buffer containing several protease inhibitors (1% Triton X-100, 50 mM Tris-HCl pH 7.4, 140 mM NaCl, 1 mM EDTA, 1 mM EGTA, 1 mM dithiothreitol (DTT), 1 mM phenylmethanesulfonyl fluoride (PMSF), 10 mM sodium fluoride (NaF), 5 mM iodoacetic acid (IAA), and 10 µg/ml of aprotinin, leupeptin, and pepstatin each). All inhibitors used were purchased from Boehringer Mannheim GmbH (Mannheim,

Germany) with the following exceptions: DTT, PMSF, and NaF, which were purchased from Sigma-Aldrich (St. Louis, MO, USA), and IAA, which was bought from ICN Biomedicals (Irvine, CA, USA). Extracts were incubated for 30 minutes on ice, centrifuged at 12000 rpm at 4°C, and the supernatants recovered. Nuclear extracts for YAP were prepared according to Timchenko *et al.* (1996). The protein concentration of the resulting total and nuclear extracts was determined according to the Bradford method (Bradford, 1976) using bovine serum albumin (BSA) (Cat. No. A9647, Sigma-Aldrich, St. Louis, MO, USA) as standard. For immunoblot analysis, equal amounts (from 100 to 150 µg/lane) of proteins were electrophoresed on 8 to 12% sodium dodecyl sulfate polyacrylamide (SDS-PAGE) homogenous gels (Cat. No. L4522, Sigma-Aldrich, St. Louis, MO, USA and Cat. No. 161-0156, Bio-Rad Laboratories, Hercules, CA, USA). After gel electrotransfer onto nitrocellulose membranes (Cat. No. 162-0097, Bio-Rad Laboratories, Hercules, CA, USA) at 300 mA overnight or 800 mA for 2 to 4 hours, to ensure equivalent protein loading and transfer in all lanes, the membranes and gels were stained with 0.5% (w/v) Ponceau S dye (Cat. No. 02190644, ICN Biomedicals, Irvine, CA, USA) in 1% acetic acid for 5 minutes, and with Coomassie Brilliant Blue (Cat. No. 04808274, ICN Biomedicals, Irvine, CA, USA) in 10% acetic acid for 30 minutes, respectively. After blocking with 5% non-fat dry milk or 5% BSA in Tris-buffered saline containing 0.05% Tween 20 (TBST) (Cat. No. P7949, Sigma-Aldrich, St. Louis, MO, USA) at room temperature for 1 hour or overnight at 4°C, membranes were washed in TBST and then incubated with the appropriate primary antibodies diluted in blocking buffer. Whenever possible, the same membrane was used for detection of the expression of different proteins. Depending on the origin of primary antibody, filters were incubated at room temperature with either anti-mouse or anti-rabbit horseradish peroxidise-conjugated IgG (Cat. No. sc-2806 and sc-2808, Santa Cruz Biotechnology, Santa Cruz, CA, USA). Immunoreactive bands were identified with SuperSignal® West Pico Chemiluminescent Substrate, as described by the manufacturer (Cat. No. 34080, Pierce, Rockford, IL, USA). The relative proportions of each sample were then estimated by densitometric analysis of the intensity of each band by using the image analysis software ImageJ (NIH, Bethesda, MD, USA).

Primary antibodies used for immunoblotting were the following: mouse monoclonal antibodies directed against actin (AC40) (Cat. No. A4700, Sigma-Aldrich, St. Louis, MO, USA), cyclin D1 (72-13G), proliferating cell nuclear antigen (PCNA) (PC10) (Cat. No. sc-450 and sc-56, Santa Cruz Biotechnology, Santa Cruz, CA, USA), and β-catenin (Clone 14) (Cat. No. 610154, BD Transduction Laboratories, San Diego, CA, USA); and rabbit polyclonal antibodies against cyclin A (C-19) (Cat. No. sc-596, Santa Cruz Biotechnology, Santa Cruz, CA, USA), and YAP (Cat. No. 4912, Cell Signaling Technology, Beverly, MA, USA).

3.5 - DNA sequencing

Total DNA was purified from frozen liver samples using QIAamp® DNA Mini Kit (Cat. No. 51304, Qiagen GmbH, Hilden, Germany). The quantity of the DNA samples was measured using a NanoDrop ND-1000 Spectrophotometer (Thermo Fisher Scientific, Wilmington, DE, USA) and the quality was assessed by calculating the ratio of absorbance at 260 nm to absorbance at 280 nm (A_{260}/A_{280} ratio). Polymerase chain reaction (PCR) was conducted in a 50 µl reaction volume containing 500 ng of DNA, 10X *Taq* Buffer with KCl, 10 mM dNTP mixture, 10 µM of each primer, and 1 U of *Taq* DNA Polymerase (Cat. No. EP0404, Fermentas GmbH, St. Leon-Rot, Germany). GeneAmp® PCR System 9700 thermal cycler (Applied Biosystems, Foster City, CA, USA) was programmed with an initial denaturation time of 5 minutes at 95°C, followed by 35 cycles with denaturation at 95°C for 1 minute, annealing 64°C/58°C/65°C (for beta-catenin 1 gene (*Ctnnb1*) primers (yielding a 1473 base pair (bp) fragment)/*Ctnnb1* primers (yielding a 248 bp fragment)/harvey rat sarcoma virus oncogene 1 gene (*Hras1*) primers (yielding a 166 bp fragment) respectively) for 1 minute, and elongation at 72°C for 1 minute. A final extension of 10 minutes at 72°C was performed. For amplification the following gene-specific primer sequences were used: *Ctnnb1* (yielding a 1473 bp fragment) - 5'-AGCTCAGCGCAGAGCTGCTG-3' (sense) and 5'-CCTTCCTGATGGAGCAGGAGA-3' (antisense); *Ctnnb1* (yielding a 248 bp fragment) - 5'-ACTCTGTTTTTACAGCTGACC-3' (sense) and 5'-

TTTACCAGCTACTTGCTCTTG-3' (antisense); *Hras1* (yielding a 166 bp fragment) - 5'-GAGACATGTCTACTGGACATCTT-3' (sense) and 5'-GCTAGCCATAGGTGGCTCACCTG-3' (antisense). Amplification products were loaded on a 2% agarose gel (Cat. No. A5093, Sigma-Aldrich, St. Louis, MO, USA) or a 10% polyacrylamide gel (Cat. No. 3029, Carl Roth GmbH, Karlsruhe, Germany), depending on the length of the resulting fragments. DNA bands were then stained with bromophenol blue (Cat. No. B0126, Sigma-Aldrich, St. Louis, MO, USA) and visualized with ethidium bromide solution (Cat. No. 46067, Sigma-Aldrich, St. Louis, MO, USA) on a MacroVue UVis-20 transilluminator (Hoefer, San Francisco, CA, USA) to make sure that the desired amplification product was obtained. PCR products were sequenced in both directions using the same primers employed for amplification on a 3730*xl* DNA Analyzer (96-capillary array) (Applied Biosystems, Foster City, CA, USA) by BMR Genomics (Padua, Italy). Nucleotide sequences were analyzed using the software ChromasPro Version 1.5 (Technelysium Pty Ltd, Tewantin, QLD, Australia).

3.6 - Restriction fragment length polymorphism (RFLP)

The previous amplification product (166 bp fragment) obtained by the *Hras1* primers was used with the following specific restriction endonucleases.

The specific restriction enzyme digest for the single base substitution sequence 'CAT' was conducted in a 20 µl reaction volume containing 800 ng of DNA, 1X NEBuffer 4 (Cat. No. B7004, New England BioLabs GmbH, Frankfurt, Germany) and 10 U of *BspHI* enzyme (Cat. No. R0517, New England BioLabs GmbH, Frankfurt, Germany) at a temperature of 37°C for 60 minutes. Moreover, digestion for the point mutated sequence 'CGA' was carried out in a 20 µl reaction volume consisting of 800 ng of DNA and 10 U of *TaqI* enzyme (Cat. No. ER0671, Fermentas GmbH, St. Leon-Rot, Germany) at a temperature of 65°C for 60 minutes. Likewise, that for the 'CTA' mutated sequence was done in a 20 µl reaction volume including 800 ng of DNA and 20 U of *XbaI* enzyme (Cat. No. R0145, New England BioLabs GmbH, Frankfurt, Germany) at a temperature of 37°C for 60 minutes. In addition, enzyme digest for the single base

substitution sequence 'AAA' was conducted in a 20 µl reaction volume composed of 800 ng of DNA, 1X NEBuffer 4, 1X BSA and 5 U of *Hpy188III* enzyme (Cat. No. R 0622, New England BioLabs GmbH, Frankfurt, Germany) at a temperature of 37°C for 20 hours. Digestion products were loaded on a 10% polyacrylamide gel, stained with bromophenol blue and visualized with ethidium bromide solution on a MacroVue UVis-20 transilluminator. Analysis of the presence of DNA fragments of different lengths was done with the help of GeneRuler™ 100 bp Plus DNA Ladder (Cat. No. SM0321, Fermentas GmbH, St. Leon-Rot, Germany). The presence of the following fragments lengths in the various enzyme digestion reactions indicated single base substitutions:

Restriction Enzyme	**Digestion Site**	**DNA Fragment/s**	
		Wild Type CAA	**Point Mutation** CAT/CGA/CTA/AAA
BspHI	5'…T|CATGA…3' 3'…AGTAC|T…5'	166 bp	130 bp + 36 bp
Taq I	5'…T|CGA…3' 3'…AGC|T…5'	125 bp + 41 bp	89 bp + 41 bp + 36 bp
XbaI	5'…T|CTAGA…3' 3'…AGATC|T…5'	166 bp	130 bp + 36 bp
Hpy188III	5'…TC|NNGA…3' 3'…AGNN|CT…5'	129 bp + 35 bp	166 bp

A positive control was included in each specific restriction enzyme digest to make sure that the specific restriction endonucleases completed their digestion.

3.7 - Quantitative reverse transcription polymerase chain reaction (qRT-PCR)

3.7.1 - Analysis of miRNA

Total RNA was extracted from frozen liver samples using Trizol® Reagent (Cat. No. 15596, Invitrogen, Carlsbad, CA, USA). The quantity of the RNA samples was measured using a NanoDrop ND-1000 Spectrophotometer and the quality was assessed by migration of RNA on agarose gel. Complementary DNA (cDNA) was synthesized using the TaqMan® MicroRNA Reverse Transcription Kit (Cat. No. 4366596, Applied Biosystems, Foster City, CA, USA) in accordance with the manufacturer's instructions. qRT-PCR amplification was performed with the reverse transcription product, TaqMan® 2X Universal PCR Master Mix, No AmpErase® UNG (Cat. No. 4324018, Applied Biosystems, Foster City, CA, USA), miRNA-375 primers and probe mix (Cat. No. 4373027, Applied Biosystems, Foster City, CA, USA), which was incubated in a 96-well plate at 95°C for 10 minutes, followed by 40 cycles of 95°C for 15 seconds each and 60°C for 1 minute, respectively on a 7300 Real-Time PCR System (Applied Biosystems, Foster City, CA, USA). The endogenous control snoRNA202 (Cat. No. 4380914, Applied Biosystems, Foster City, CA, USA) was used to normalize miRNA expression levels.

3.7.2 - Analysis of messenger RNA (mRNA)

2 μg of total RNA, extracted with RNeasy® Plus Mini Kit (Cat. No. 74134, Qiagen GmbH, Hilden, Germany), was reverse transcribed using the High-Capacity cDNA Reverse Transcription Kit (Cat. No. 4374966, Applied Biosystems, Foster City, CA, USA) according to the manufacturer's protocol. cDNA together with TaqMan® Gene Expression Master Mix (Cat. No. 4369016, Applied Biosystems, Foster City, CA, USA), CAR primers and probe mix (Cat. No. Mm00437986_m1, Applied Biosystems, Foster City, CA, USA), Cyp2b10 primers and probe mix (Cat. No. Mm00456591_m1, Applied Biosystems, Foster City, CA, USA), Birc5 primers and probe mix (Cat. No. Mm00599749_m1, Applied Biosystems, Foster City, CA, USA), or AFP primers and probe mix (Cat. No. Mm00431715_m1, Applied Biosystems, Foster City, CA, USA) was used to carry out qRT-PCR amplification. The thermal cycling conditions were 50°C for 2 minutes, 95°C for 10 minutes, followed by 40 cycles of 95°C for 15 seconds

each and 60°C for 1 minute, respectively. Glyceraldehyde-3-phosphate dehydrogenase (GAPDH) (Cat. No. 4352932E, Applied Biosystems, Foster City, CA, USA) was used as the endogenous normalizer.

In both procedures, the relative amount of miRNA/mRNA was determined with the $2^{-\Delta\Delta CT}$ method, where $\Delta\Delta C_T = (C_{T\ target} - C_{T\ endogenous})_{sample} - (C_{T\ target} - C_{T\ endogenous})_{calibrator}$.

3.8 - Semiquantitative reverse transcription polymerase chain reaction (sqRT-PCR)

sqRT-PCR was conducted in a 50 µl reaction volume containing 50 ng of cDNA, 10X High Fidelity PCR Buffer, 50 mM $MgSO_4$, 10 mM dNTP mixture, 5 µM of each primer, and 1 U of Platinum® *Taq* DNA Polymerase High Fidelity (Cat. No. 11304, Invitrogen, Carlsbad, CA, USA). GeneAmp® PCR System 9700 thermal cycler was programmed with an initial denaturation time of 5 minutes at 94°C, followed by an appropriate number of cycles with denaturation at 94°C for 30 seconds, annealing at 58°C for 30 seconds, and elongation at 72°C for 1 minute. A final extension of 5 seconds at 72°C was performed. Thirty-two and twenty cycles were found to be optimal for CTGF and 18S, respectively. For amplification the following gene-specific primer sequences were used: CTGF - 5'-GCGCCAAGCAGCTGGGAGAA-3' (sense) and 5'-GCAGCTAGGGCAGGGCCAAC-3' (antisense); 18S - 5'-AAACGGCTACCACATCCAAG-3' (sense) and 5'-CCCTCTTAATCATGGCCTCA-3' (antisense). The PCR products were loaded on 2% agarose gel, stained with bromophenol blue and visualized with ethidium bromide solution on a MacroVue UVis-20 transilluminator. The relative proportions of each sample were then estimated by densitometric analysis of the intensity of each band by using the image analysis software ImageJ.

3.9 - Statistical analysis

Instant statistics software (GraphPad InStat Software Inc., San Diego, CA, USA) was used to analyze the data. The results of multiple observations were presented as the mean ± standard error (SE) of at least two separate experiments. A *P* value of <0.05 was regarded as a significant difference between groups.

Chapter 4

Results and Discussion

4.1 - Effect of repeated doses of TCPOBOP on hepatocyte proliferation in a normal liver

TCPOBOP is a well known powerful inducer of hepatocyte proliferation in mice (Dragani *et al.*, 1985; Manenti *et al.*, 1987), when administered in a single dose, nevertheless no evidence has been provided about its effect on the liver size following repeated administration. For this purpose, **Experimental Protocol I** was designed.

Statistical analyses showed that a single injection of TCPOBOP was able to induce doubling of the liver mass in a week (10.96 ± 0.27% *vs.* 5.31 ± 0.08% of control animals), but the same cannot be said after the second dose, where the difference in liver mass, when compared to the first dose group, was almost negligible (11.39 ± 0.19% *vs.* 10.96 ± 0.27%) (**Fig. 8**). The increase in liver mass observed after the first dose of the mitogen was largely due to hepatocyte proliferation, as shown by a striking increase in percentage of BrdU-positive nuclei in mice receiving the first dose of TCPOBOP when compared to their respective controls (43.95 ± 1.88% *vs.* 3.83 ± 0.57%). On the contrary, there was no significant hepatocyte proliferation in mice treated with a second dose of the mitogen when compared to control animals (5.91 ± 0.86% *vs.* 3.83 ± 0.57%) (**Fig. 9, 10**).

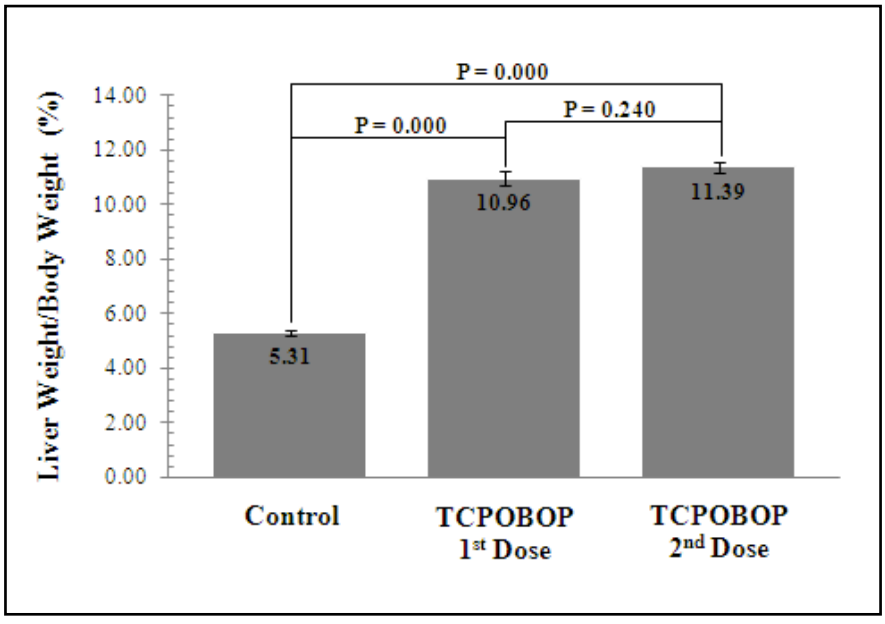

Fig. 8 Percentage of liver to body weight in mice belonging to the various groups described in Experimental Protocol I. Results are expressed as means ± SE of five mice per group.

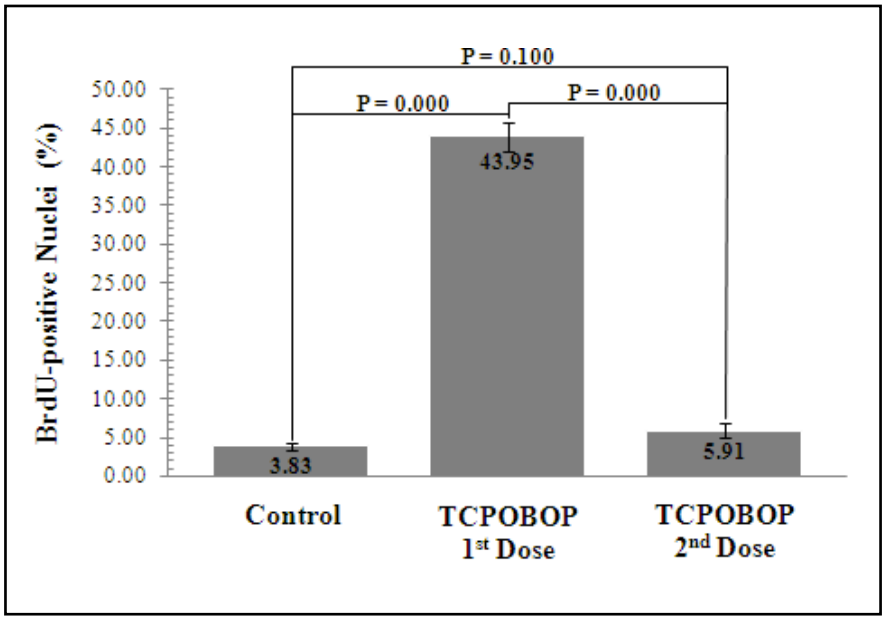

Fig. 9 Percentage of BrdU-positive nuclei in liver sections of mice belonging to the various groups described in Experimental Protocol I. Results are expressed as means ± SE of five mice per group.

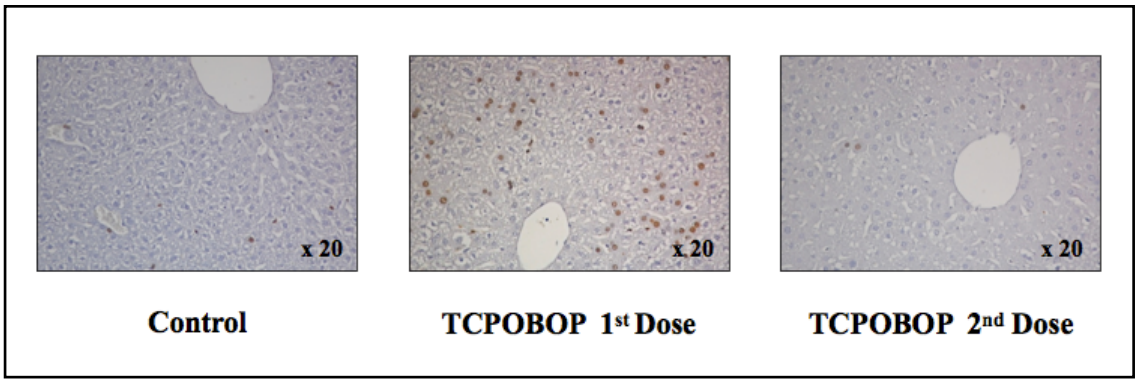

Fig. 10 Representative microscopic view of liver sections from mice belonging to the various groups described in Experimental Protocol I stained immunohistochemically for BrdU (original magnification x 20).

Such analyses made it clear that hepatocytes receiving a second dose of TCPOBOP a week after the first dose were not able to proliferate at the same rate as those receiving a single dose of the mitogen.

4.1.1 - Xenobiotic metabolism following repeated administration of the mitogen

TCPOBOP is an agonist ligand for the nuclear receptor CAR. The protein binds to DNA as a monomer or a heterodimer with the RXR and induces the transcription of target genes implicated in drug metabolism, such as CYP family members, especially Cyp2b10 (Poland *et al.*, 1980; Tzameli *et al.*, 2000). In order to clarify if the absence of a significant hepatocyte proliferation response following repeated treatments with TCPOBOP was related to a xenobiotic metabolism issue, qRT-PCR analysis of CAR and Cyp2b10 mRNAs was performed.

Statistical interpretation showed that the relative quantity (RQ) of CAR mRNA in the livers of mice injected with the first dose of TCPOBOP, when compared to the respective controls, was considerably decreased (0.27 ± 0.01 *vs.* 1.01 ± 0.10). Similarly, when livers treated with a second dose of the mitogen were compared to the control group, the relative amount of CAR mRNA was equally repressed (0.30 ± 0.03 *vs.* 1.01 ± 0.10). Since variation in the downregulation of this nuclear receptor in livers treated with one or two doses of the mitogen was insignificant, it was assumed that the agonist effect of TCPOBOP was identical in both groups (**Fig. 11**). Moreover, evaluation of Cyp2b10 mRNA relative quantities demonstrated that there was a notable upregulation after administration of the mitogen (27.33 ± 3.08 after the first dose of TCPOBOP / 29.02 ± 2.98 after the second dose of TCPOBOP *vs.* 1.00 ± 0.09 of controls). The difference in the increased expression of this target gene was negligible in livers administered with one or two doses of the mitogen, indicating that Cyp2b10 induction was equal in both treated groups. This confirms that TCPOBOP was metabolized at the same extent after the respective doses, hence the mitogenic effect should be alike (**Fig. 12**).

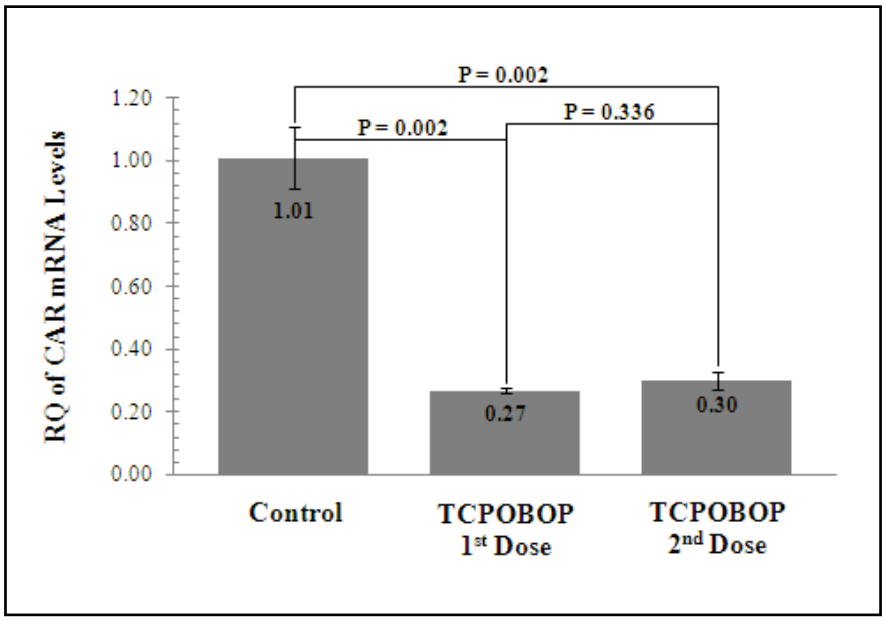

Fig. 11 RQ of CAR mRNA levels in livers of mice belonging to the various groups described in Experimental Protocol I, determined by qRT-PCR analysis. GAPDH was used as an endogenous normalizer. Results are expressed as means ± SE of three livers per group.

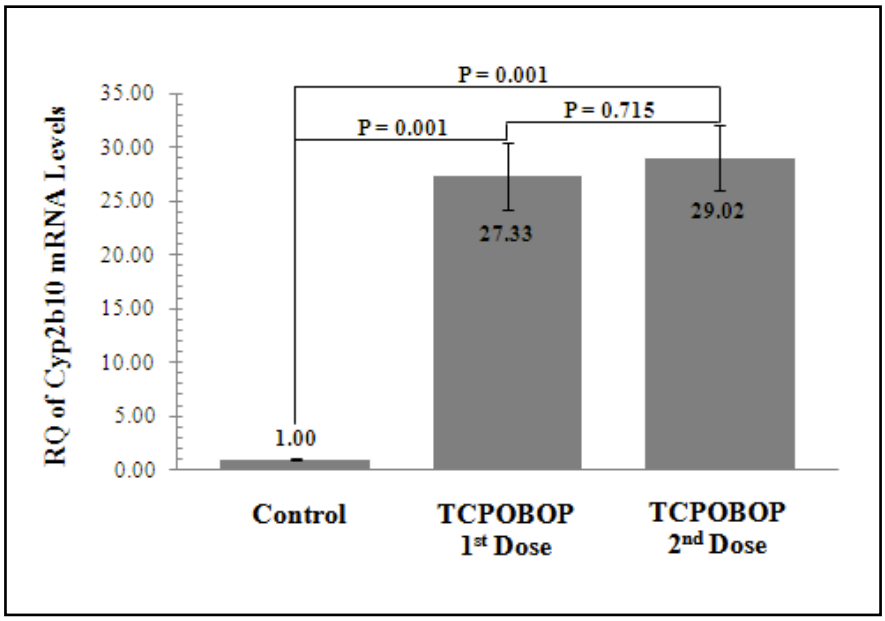

Fig. 12 RQ of Cyp2b10 mRNA levels in livers of mice belonging to the various groups described in Experimental Protocol I, determined by qRT-PCR analysis. GAPDH was used as an endogenous normalizer. Results are expressed as means ± SE of three livers per group.

4.1.2 - Time interval issue for hepatocytes to reply to a further mitogenic stimulus

In order to elucidate if the refractory effect on hepatocyte proliferation, observed after the second dose of TCPOBOP, was related to a short time interval between the two doses, thus rendering hepatocytes unable to further respond to the mitogen, another similar protocol, consisting of the same previous experimental groups, was set up with the exception that the time period between the first and second dose of TCPOBOP was of 4 weeks instead of 1 week (**Experimental Protocol II**).

Statistical evaluation of the percentage liver to body weight confirmed approximately the same results obtained with the previous experimental protocol. Particularly, the first dose of TCPOBOP was able to increase the liver weight by a twofold (10.02 ± 0.26% *vs.* 5.02 ± 0.09% of control animals), while the second dosage resulted in a slightly bigger liver, when compared to the first dose group, although not statistically significant (10.63 ± 0.14% *vs.* 10.02 ± 0.26%) (**Fig. 13**).

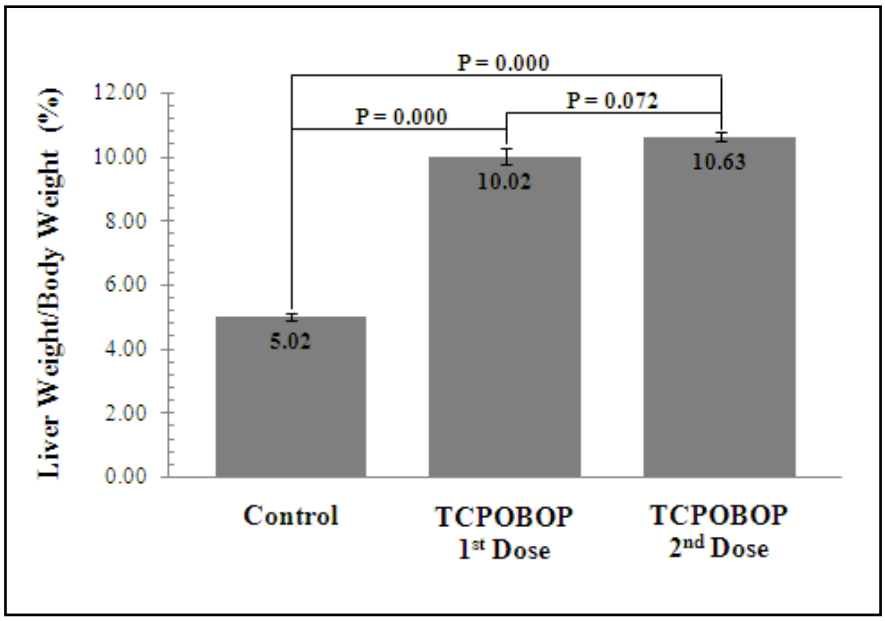

Fig. 13 Percentage of liver to body weight in mice belonging to the various groups described in Experimental Protocol II. Results are expressed as means ± SE of five mice per group.

Similarly to what was observed in Experimental Protocol I, immunohistochemical analyses of the percentage BrdU-positive nuclei showed that the first administration of TCPOBOP resulted in a staggering surge of BrdU-incorporation when compared to the control group (40.19 ± 2.44% *vs.* 4.18 ± 0.42%), while the rate of proliferation was still much lower with two doses of the mitogen, although there was a considerable increase in hepatocyte proliferation compared to control animals (13.16 ± 1.17% *vs.* 4.18 ± 0.42%) (**Fig. 14**).

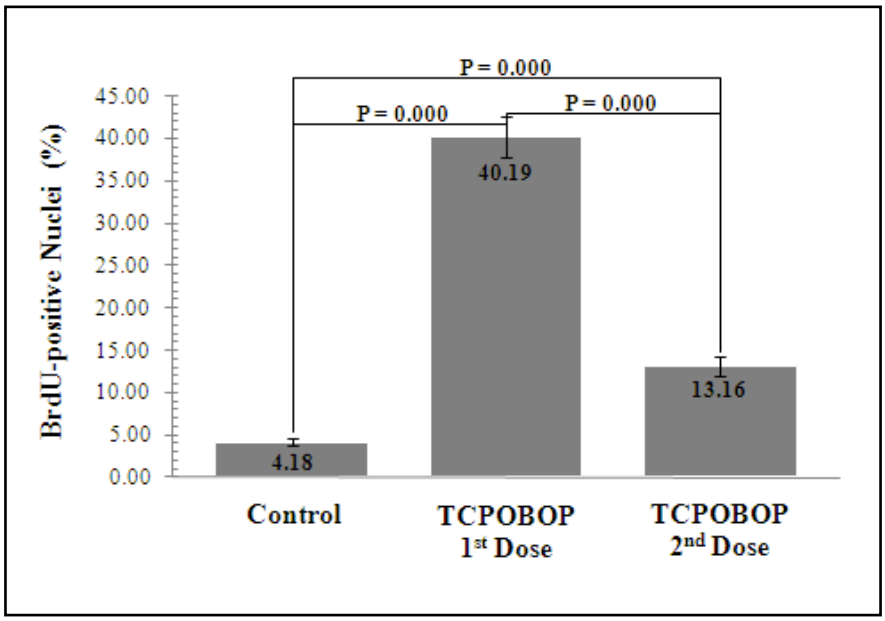

Fig. 14 Percentage of BrdU-positive nuclei in liver sections of mice belonging to the various groups described in Experimental Protocol II. Results are expressed as means ± SE of five mice per group.

This study demonstrates that a longer time period between the two doses did not actually change the proliferation response of the hepatocytes following repeated treatments with the same mitogen.

4.2 - Role of the Hippo pathway in liver refractoriness to repeated administration of TCPOBOP

Recent studies on organ size control reported, in both *Drosophila* and mammals, the critical role of Hippo kinase cascade, a growth-suppressive pathway that ultimately antagonises the transcriptional coactivator YAP (Camargo *et al.*, 2007; Dong *et al.*, 2007). Hence, to investigated whether Hippo pathway activation might be the homeostatic mechanism responsible for the liver refractoriness to further challenge of the mitogen **Experimental Protocol III** was carried out.

Statistical analyses of this kinetic study supported the previous results, in that, the liver mass peaks a week after the first administration of TCPOBOP (11.64 ± 0.23% *vs*. 5.77 ± 0.14% of control animals), but further growth ceases following a second dose of the mitogen (11.30 ± 0.09% / 11.85 ± 0.11% 24 and 36 hours after the second dose of TCPOBOP *vs.* 11.64 ± 0.23% of control animals) (**Fig. 15**). It was also confirmed that hepatocyte proliferation was responsible for the significant increase in liver mass noticed after the first dose of the mitogen with percentage of BrdU-positive nuclei peaking after 36 hours (30.88 ± 0.96% *vs.* 2.86 ± 1.11% of controls). Moreover, according to previous data, it was shown that after the second administration of TCPOBOP, hepatocyte proliferation was negligible, when compared to control animals (2.25 ± 0.62% / 4.05 ± 0.09% 24 and 36 hours after the second dose of the mitogen *vs.* 2.86 ± 1.11% of controls) (**Fig. 16**).

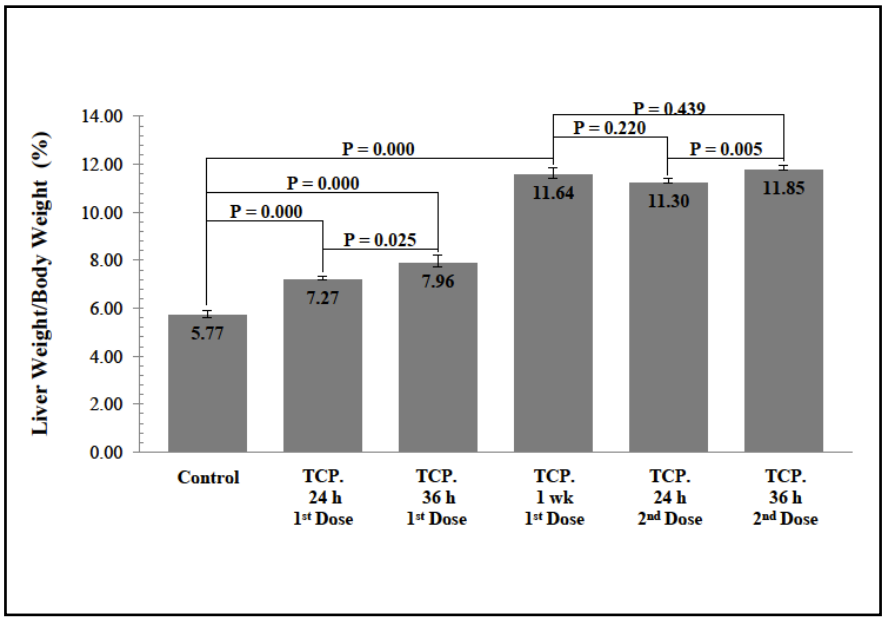

Fig. 15 Percentage of liver to body weight in mice belonging to the various groups described in Experimental Protocol III. Results are expressed as means ± SE of five mice per group.

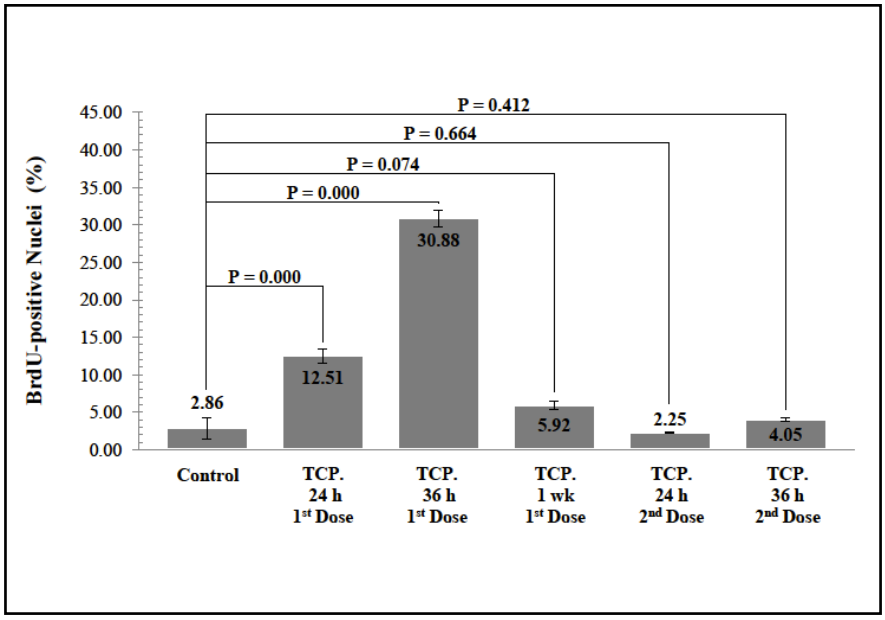

Fig. 16 Percentage of BrdU-positive nuclei in liver sections of mice belonging to the various groups described in Experimental Protocol III. Results are expressed as means ± SE of five mice per group.

The increased hepatocyte entry into the S phase, observed by BrdU staining in liver sections of mice receiving a single dose of TCPOBOP, was associated with enhanced levels of the cell cycle-related proteins, cyclin D1, cyclin A and PCNA, all indicators of proliferation when overexpressed (Pines, 1995). Oppositely, after the second dose of TCPOBOP, no such increase was noticed, in conformity with the previously observed inhibitory effect response on hepatocyte proliferation exerted by the second dose of the same mitogen (**Fig. 17**).

Accordingly to its growth promoting effect, Western Blot analysis indicated substantially higher levels of YAP after a single dose of TCPOBOP. On the contrary, no increase of YAP levels was noticed after the second dose of the mitogen (**Fig. 17**), presumably as a consequence of the activation of the Hippo growth-suppressive pathway, leading to YAP phosphorylation, thus, inactivation of the protein.

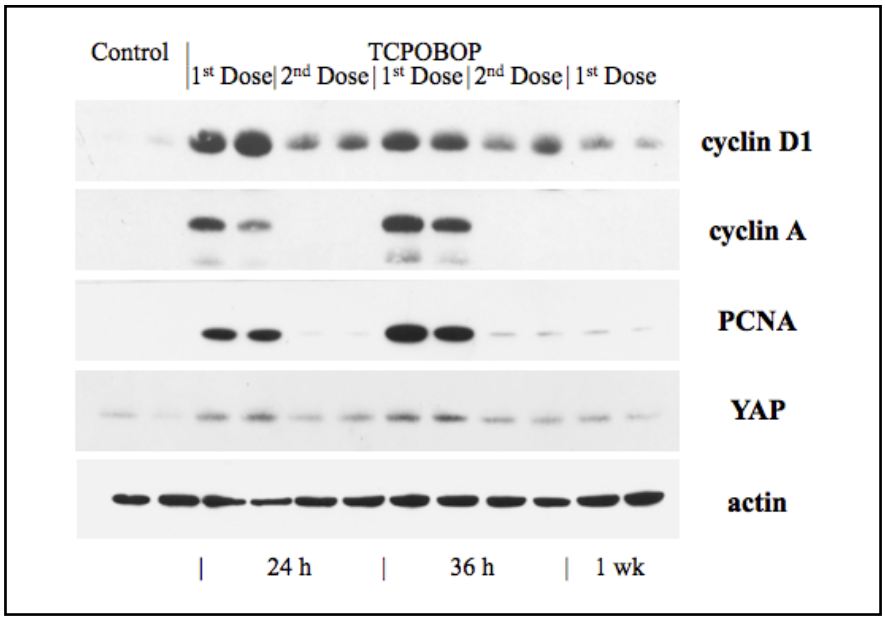

Fig. 17 Levels of cyclin D1, cyclin A, PCNA and YAP in total hepatic protein extracts of mice belonging to the various groups described in Experimental Protocol III, determined by Western Blot analysis. Actin was used as a loading control. Each lane represents a single sample.

As reported in the literature, YAP induces the transcription of many target genes, among which of remarkable importance is Birc5/survivin, a member of the inhibitor of apoptosis (IAP) gene family, which encode negative regulatory proteins that prevent apoptotic cell death (Dong *et al.*, 2007; Hao *et al.*, 2008). qRT-PCR analysis demonstrated that the mRNA expression of Birc5 was positively correlated with the expression of YAP protein, since a twenty-fold increase of Birc5 36 hours after the first dose of TCPOBOP was observed, whereas only a two-fold change was noticed after the second dose of the mitogen when compared to the control group (**Fig. 18**). These results further support the involvement of YAP, thus of the Hippo signaling pathway, in TCPOBOP-induced hepatocyte proliferation.

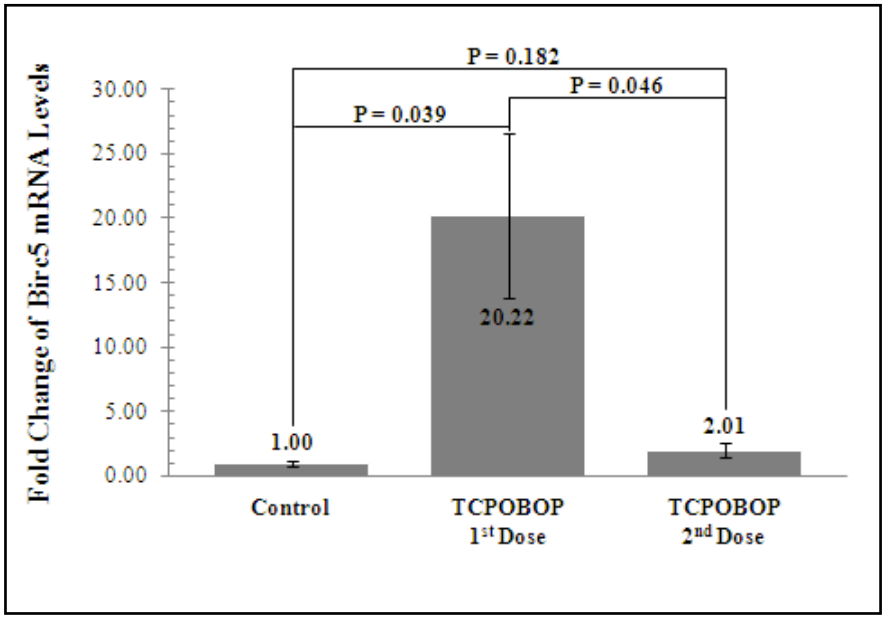

Fig. 18 Fold change of Birc5 mRNA levels in livers of mice belonging to the various groups described in Experimental Protocol III, determined by qRT-PCR analysis. GAPDH was used as an endogenous normalizer. Results are expressed as means ± SE of three livers per group.

4.3 - Analysis of tumor incidence at various time points during DENA + TCPOBOP-induced carcinogenesis

TCPOBOP, other than being able to induce hepatomegaly after a single dose, can also act as a non-genotoxic liver carcinogen following chronic administration (Dragani *et al.*, 1985; Dragani *et al.*, 1987; Diwan *et al.*, 1992). Therefore, **Experimental Protocol IV** was conducted to investigate in TCPOBOP-dependent carcinogenesis if DENA-induced mutations allow 'initiated' hepatocytes to selectively 'escape' from such an organ constraint, related to administration of repeated doses of the mitogen, thus favoring their clonal expansion and eventually leading to HCC.

Percentage of liver to body weight at the 10-week time period demonstrated that while there was a two-fold increase in TCPOBOP treated livers when compared to those exposed to DENA only (11.87 ± 0.13% *vs.* 5.02 ± 0.10%), no remarkable difference between the TCPOBOP and DENA + TCPOBOP group was observed (11.87 ± 0.13% *vs.* 11.36 ± 0.16%) (**Fig. 19**). Moreover, the liver to body weight ratio at the 20-week time point confirmed the doubling in liver mass of the TCPOBOP group with respect to the DENA group (12.31 ± 0.20% *vs.* 4.76 ± 0.18%), although a three-fold change was seen between the DENA + TCPOBOP and DENA group (18.04 ± 1.62% *vs.* 4.76 ± 0.18%) (**Fig. 20**). In addition, percentage of liver to body weight at the 28-week time period showed a similar trend to the previous time point, with the difference that there was a five-fold increase in the DENA + TCPOBOP group when compared to the DENA group (31.57 ± 0.71% *vs.* 5.87 ± 0.48%) (**Fig. 21**). This liver weight variation between the TCPOBOP and DENA + TCPOBOP group, noticed at the 20 and 28-week time points, could be the consequence of the presence of tumors.

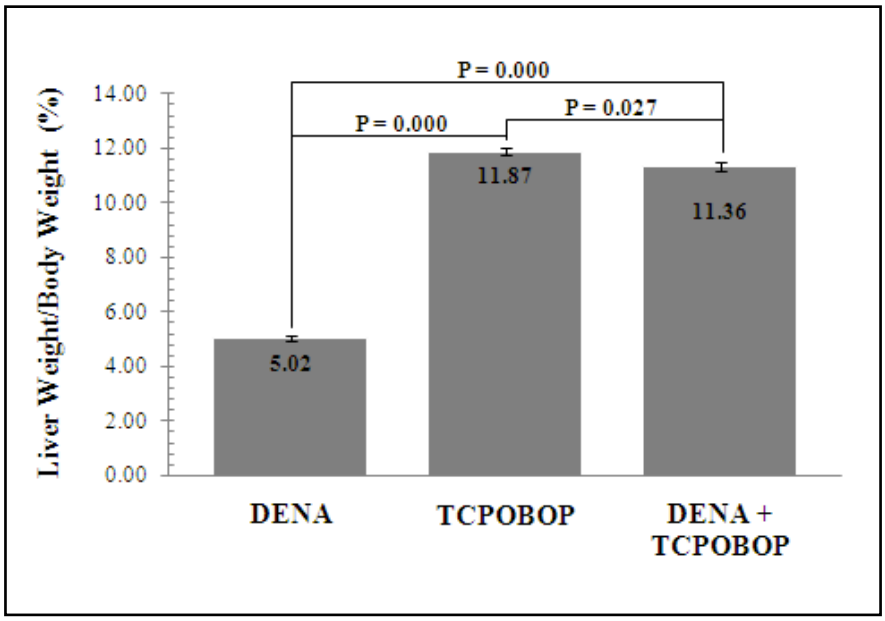

Fig. 19 Percentage of liver to body weight in mice belonging to the various 10-week time point groups described in Experimental Protocol IV. Results are expressed as means ± SE of eight mice per group.

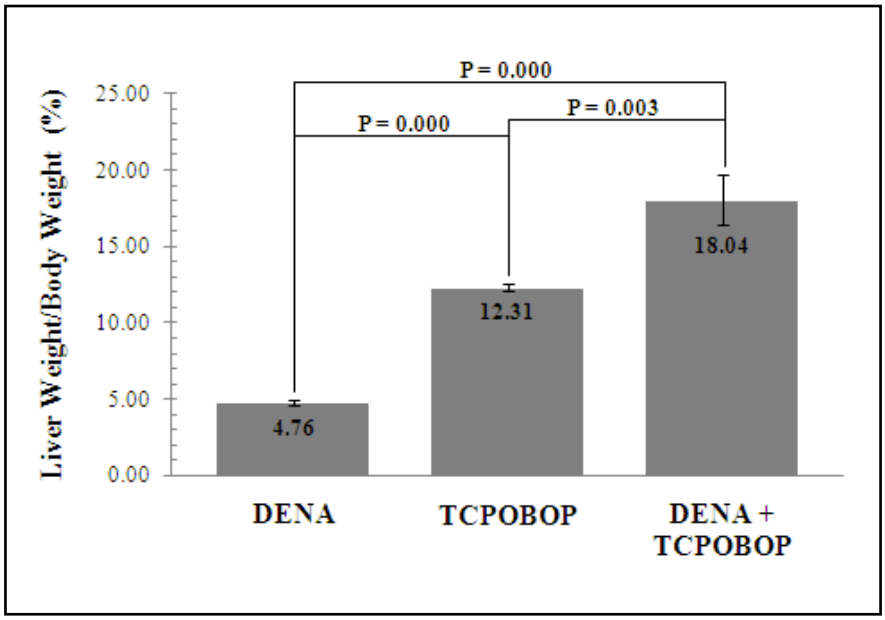

Fig. 20 Percentage of liver to body weight in mice belonging to the various 20-week time point groups described in Experimental Protocol IV. Results are expressed as means ± SE of eight mice per group.

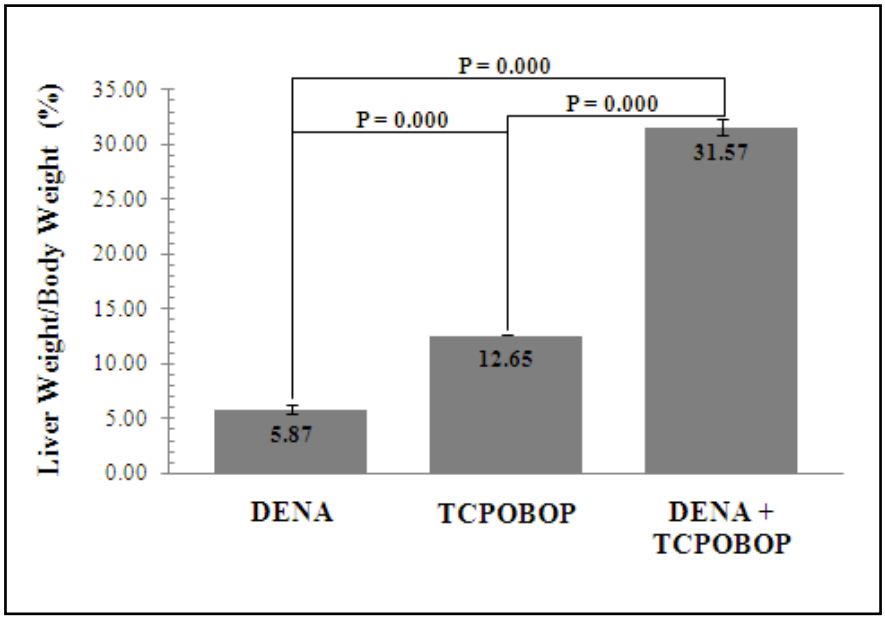

Fig. 21 Percentage of liver to body weight in mice belonging to the various 28-week time point groups described in Experimental Protocol IV. Results are expressed as means ± SE of eight mice per group.

Accordingly, macroscopic analysis showed that while after the 10-week time period there was no evidence of hepatic lesions, after the 20-week time point immediate macroscopical unifocal nodular lesions were visible in (8/8) livers of the DENA + TCPOBOP group solely. Macroscopic lesions were also perceptible in all (8/8) livers of the DENA + TCPOBOP group after the 28-week time period, but the multifocal type was more frequently found (**Fig. 22**).

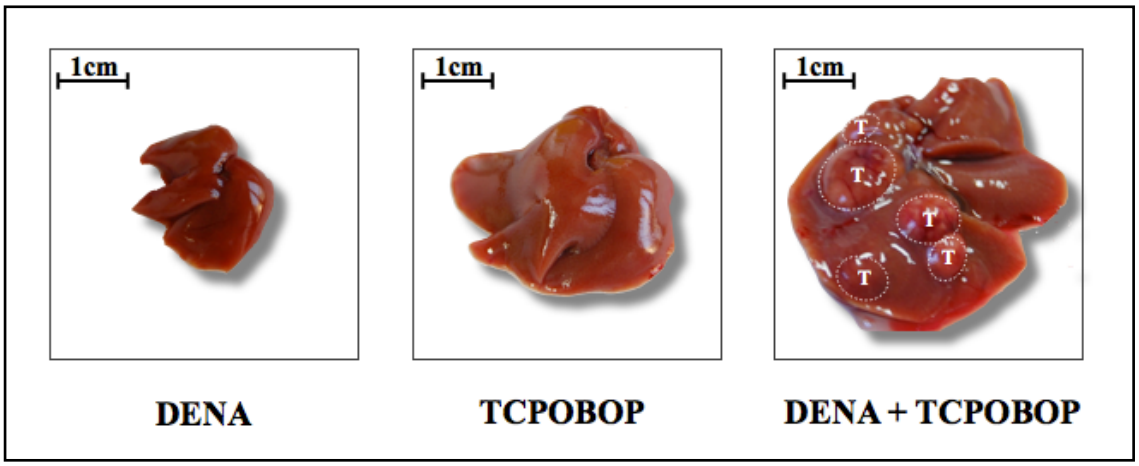

Fig. 22 Representative macroscopic view of livers from mice belonging to the various 28-week time point groups described in Experimental Protocol IV.

A total of 42 nodular lesions with an average diameter of 6.16 mm were identified in the 20-week time point livers. The left lateral lobe (assigned according to Cook, 1965) presented the highest number of nodules together with the biggest mean diameter of such nodules (**Table 3, 4**). The 28-week time period livers presented slightly less lesions (36 nodules) but with a considerably bigger mean diameter (12.89 mm), when compared to the 20-week time point livers, indicating the presence of merging nodular lesions.

	Left Lobe	**Median Lobe**	**Right Lobe**	**Caudate Lobe**
20-wk time point	24	0	13	5
28-wk time point	14	11	10	1

Table 3 Total number of nodules in the various lobes of livers from mice belonging to the DENA + TCPOBOP experimental group.

	Left Lobe	**Median Lobe**	**Right Lobe**	**Caudate Lobe**
20-wk time point	8.63 mm^2	-	3.62 mm^2	1.00 mm^2
28-wk time point	18.21 mm^2	4.45 mm^2	14.00 mm^2	20.00 mm^2

Table 4 Average diameter of nodules in the various lobes of livers from mice belonging to the DENA + TCPOBOP experimental group.

Microscopic analysis of H&E stained sections demonstrated that 84.62% of the 28-week time period livers showed trabecular nodules (classified according to Vesselinovitch *et al.*, 1978), compared to the 36.84% of the 20-week time point livers, indicating that the former lesions were in a more advanced tumor state.

Additional examination of these sections further confirmed that the 28-week time period livers exhibited notably bigger mean tumor area, when compared to the 20-week time point ones (4.93 ± 1.07 mm^2 *vs.* 1.70 ± 0.28 mm^2). Furthermore, opposite to what was

noticed with the macroscopic analysis, more tumors were observed at the 28-week time period (6.10 ± 1.08/cm^2 *vs.* 3.16 ± 0.77/cm^2 of the 20-week time point livers). This is due to the fact that merging nodular lesions under the microscope could still be distinguished. These two factors obviously contributed to a higher tumor mass in livers at the 28-week then at the 20-week time period (29.31 ± 4.59% *vs.* 5.25 ± 1.19%) (**Fig. 23**), hence confirming that the difference in liver weight previously observed between the DENA + TCPOBOP group of the 20 and 28-week time point was due to the increase in percentage tumor mass.

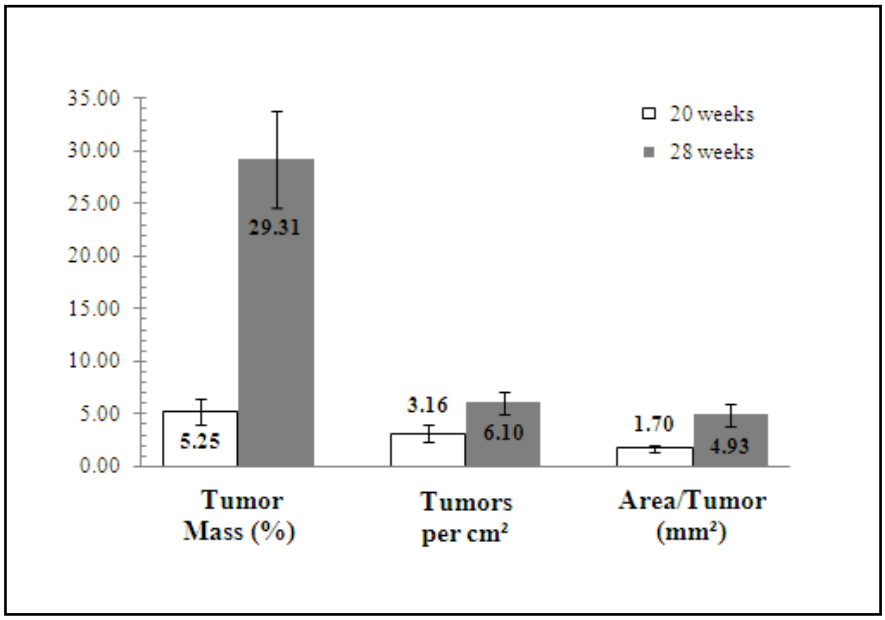

Fig. 23 Microscopic tumor analysis of liver sections from mice belonging to the 20 and 28-week time points of the DENA + TCPOBOP experimental group. Results are expressed as means ± SE of eight liver sections per time point.

Microscopic analysis of BrdU stained liver sections belonging to the 20 and 28-week time periods revealed very high proliferation in the tumor zone, while no proliferation was seen in the surrounding tissue of the DENA + TCPOBOP group; hence in concordance with the inhibitory effect exerted by repeated doses of the mitogen on hepatocyte proliferation in normal tissue, observed in the TCPOBOP group (**Fig. 24**). This explains further that the difference in liver weight between the TCPOBOP and DENA + TCPOBOP group, at the 20 and 28-week time points, was due to the

proliferating tumors in the latter group, thus confirming the hypothesis that 'initiated' hepatocytes are able to continue proliferating in spite of such organ constraint.

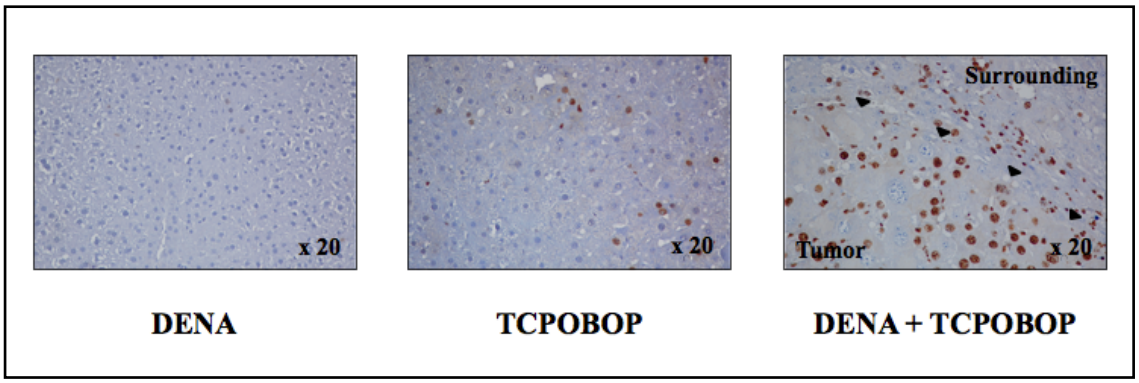

Fig. 24 Representative microscopic view of liver sections from mice belonging to the various 28-week time point groups described in Experimental Protocol IV stained immunohistochemically for BrdU (original magnification x 20).

4.4 - Role of the Hippo pathway in DENA + TCPOBOP-induced HCC

Since the mammalian Hippo circuit is not only implicated in organ size regulation but also in tumorigenesis; while its primary effector, YAP, is overexpressed and nuclearly localized in multiple types of human cancer (Overholtzer *et al.*, 2006; Steinhardt *et al.*, 2008), YAP immunohistochemistry was carried out on liver sections belonging to the 28-week time point of the DENA + TCPOBOP group. As shown in **Figure 25**, YAP was predominantly translocated in the nuclei of tumor cells, while the corresponding tissue surrounding the tumor presented primarily cytoplasmic YAP staining.

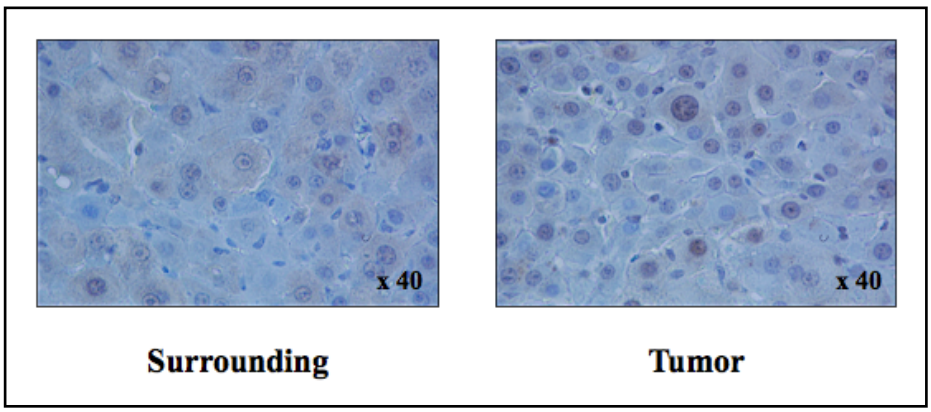

Fig. 25 Representative microscopic view of a liver section from a mouse belonging to the 28-week time point of the DENA + TCPOBOP experimental group stained immunohistochemically for YAP (original magnification x 40).

Next, the hypothetic alteration of the Hippo pathway was evaluated in the same hepatic tumors by determining YAP total protein extract levels by Western Blot analysis. Densitometric analysis showed that in approximately 80% (18/21) of tumor samples, levels of YAP increased by an average fold of two when compared to the non-tumorous surrounding tissue (**Fig. 26**). Loss of Hippo kinase cascade activity in these tumors was substantiated by an almost two-fold increase of YAP nuclear protein extract levels with respect to the normal surrounding tissue (**Fig. 27**). This confirms that cancer cells, unlike the surrounding hepatocytes, were still able to enter the cell cycle in response to repeated doses of TCPOBOP, presumably they were capable of 'escaping' from the growth-suppressive environment regulating the growth of normal hepatocytes.

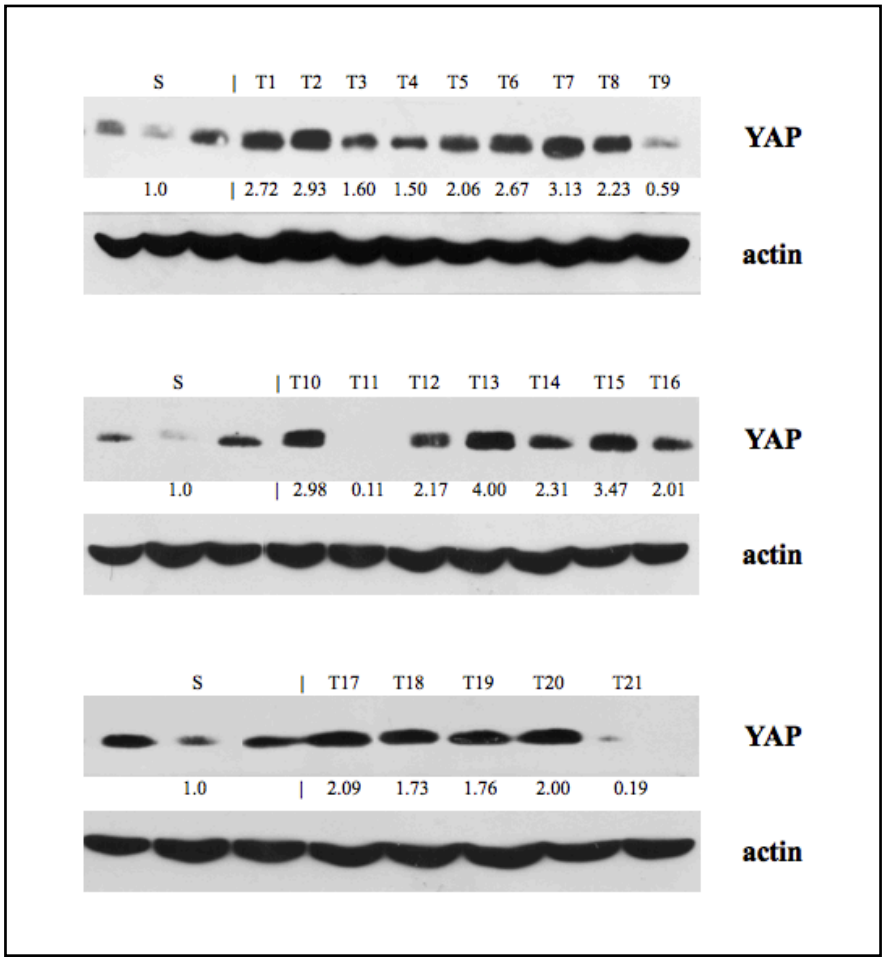

Fig. 26 Levels of YAP in total protein extracts of the various tumor samples (T) with respect to the non-tumorous surrounding liver tissue (S), determined by Western Blot analysis. Actin was used as a loading control. Each lane represents a single sample. Relative expression values determined by densitometric analysis are reported under each band.

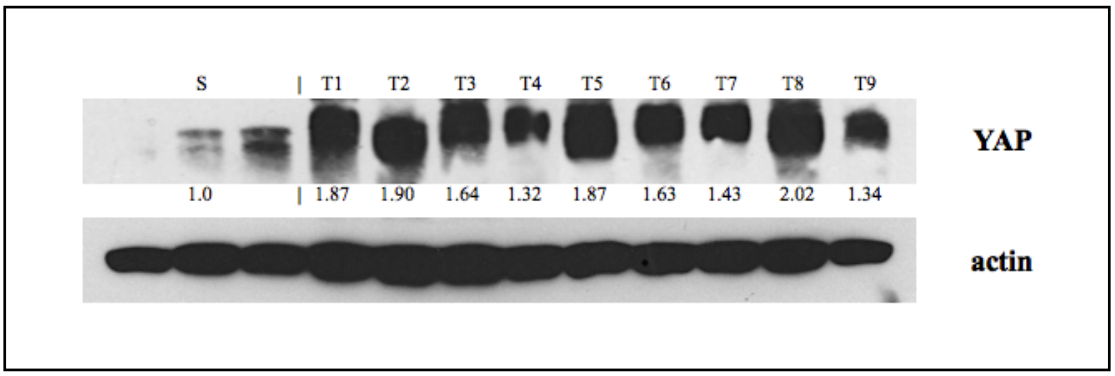

Fig. 27 Levels of YAP in nuclear protein extracts of the various tumor samples (T) with respect to the non-tumorous surrounding liver tissue (S), determined by Western Blot analysis. Actin was used as a loading control. Each lane represents a single sample. Relative expression values determined by densitometric analysis are reported under each band.

Previous studies by Dong *et al.* (2007) identified YAP-induced genes in murine livers by microarray analysis. Among the candidate genes associated with hepatocyte proliferation, AFP was classified. qRT-PCR analysis showed that in all (21/21) the tumor samples AFP transcript levels were significantly elevated by a mean fifty-fold with respect to those of the non-tumorous surrounding tissue (**Fig. 28**). Next, another direct YAP target gene required for cell growth, CTGF (Zhao *et al.*, 2007; Zhao *et al.*, 2008; Zhou *et al.*, 2009), a member of the CCN protein family, which causes a variety of cellular responses, including reduced cell adhesion and enhanced cell migration and proliferation (Brigstock, 1999), was studied in the same tumors. Data obtained showed that in nearly 60% (12/21) of the tumor samples, CTGF levels, examined by sqRT-PCR, appeared to be higher from the bands intensity, as successively confirmed by densitometric analysis (**Fig. 29**). The latter results further support the fact that in DENA + TCPOBOP-induced carcinogenesis, YAP activity dysregulation contributes to uncontrolled hepatocyte proliferation, leading ultimately to such tumor growth.

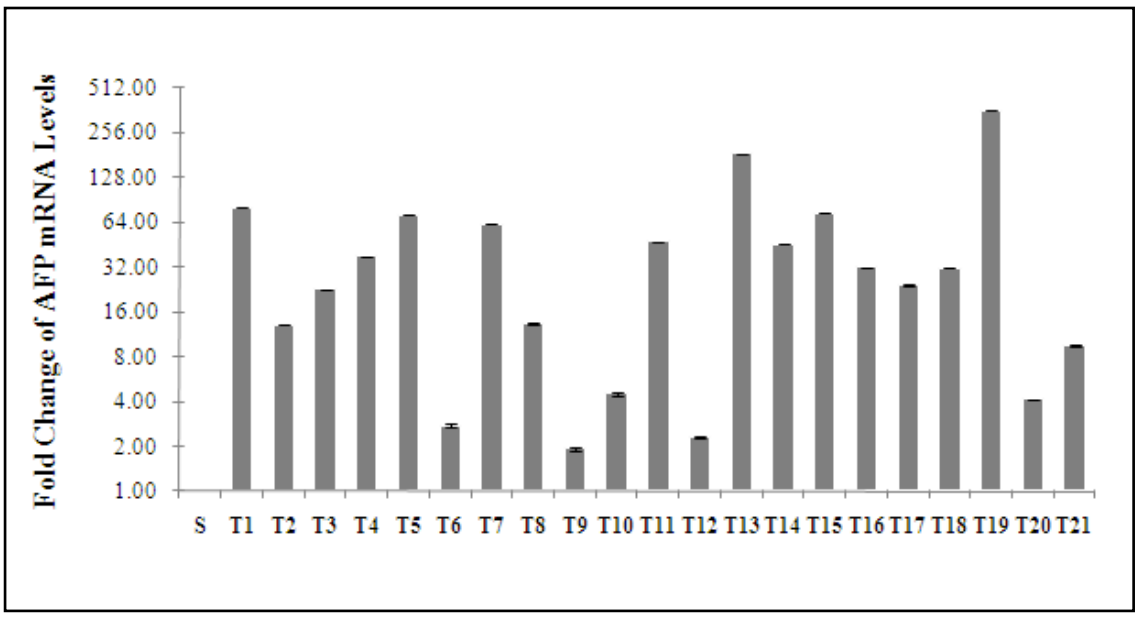

Fig. 28 Fold change of AFP mRNA levels of the various tumor samples (T) with respect to the non-tumorous surrounding liver tissue (S), determined by qRT-PCR analysis. GAPDH was used as an endogenous normalizer. Results are expressed as means ± SE of three RT-PCRs per sample.

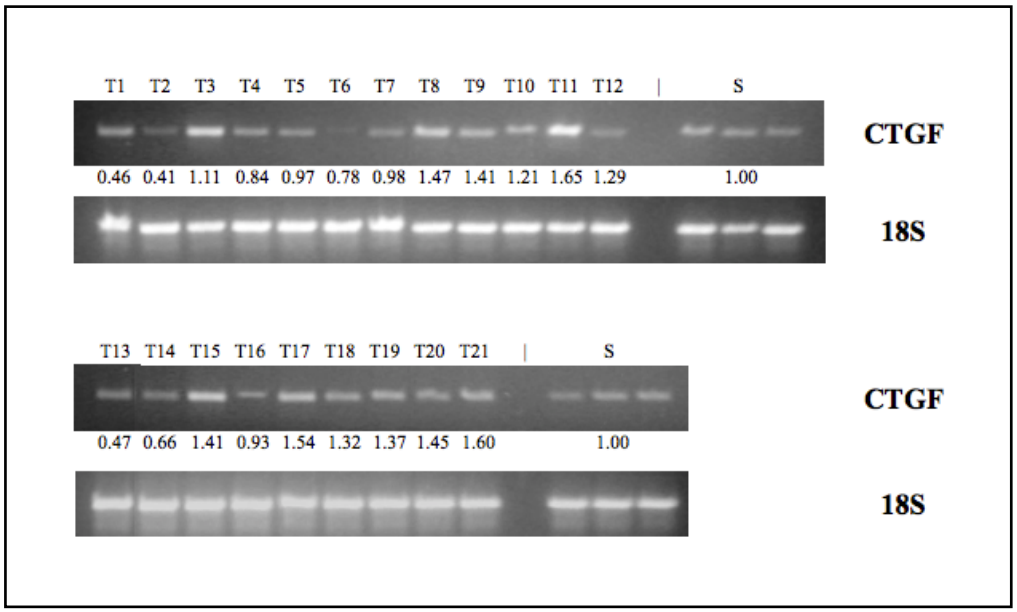

Fig. 29 mRNA levels of CTGF of the various tumor samples (T) with respect to the non-tumorous surrounding liver tissue (S), determined by sqRT-PCR analysis. 18S was used as an internal control. Each lane represents a single sample. Relative expression values determined by densitometric analysis are reported under each band.

In recent years, miRNAs have rapidly emerged as important modulators of gene expression in cancer (Iorio and Croce, 2009), including human HCC (Ladeiro *et al.*, 2008; Braconi and Patel, 2008). MiRNAs, are conserved, small (≈ 22 nucleotides), non-coding RNAs, which by pairing to complementary binding sites within the 3' untranslated region of hundred of target mRNAs, impair their translation or promote their degradation, thus participating in the control of crucial processes, such as development, cell proliferation, apoptosis, and differentiation (Ambros, 2004; Bartel, 2004; Fornari *et al.*, 2010). Signaling pathways (such as the Hippo tumor-suppressor pathway) are ideal candidates for miRNA-mediated regulation owing to the sharp dose-sensitive nature of their effects (Inui *et al.*, 2010). As a matter of fact, Liu *et al.* in 2010, reported that not only the YAP oncogene was negatively regulated by miRNA-375 but, more crucially, its downregulation was observed in tumor tissue of HCC patients, suggesting that YAP is a target of miRNA-375. To verify these findings in the previously analyzed hepatic tumors, qRT-PCR was performed to assess miRNA-375 expression. Data obtained demonstrated a significant decrease in 17 out of 21 tumors (81%) when compared to the non-tumorous surrounding tissue. Furthermore, an inverse

correlation between miRNA-375 and YAP protein was found in almost 70% (14/21) of the analyzed samples (**Fig. 30**). These results further confirm the involvement of YAP, hence the Hippo tumor-suppressor pathway, in DENA + TCPOBOP-induced HCC.

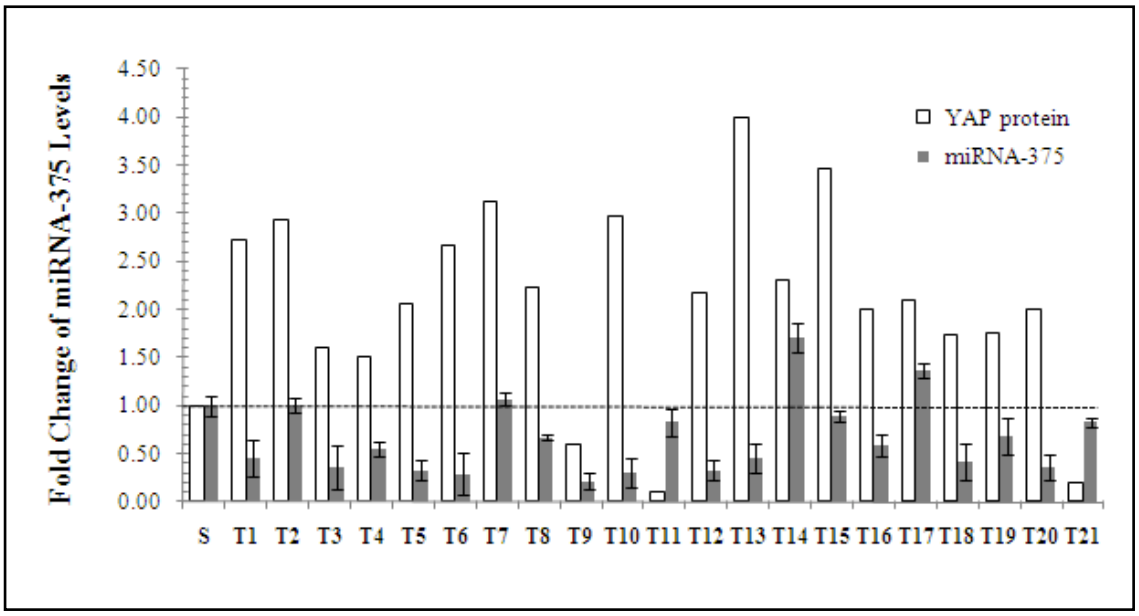

Fig. 30 Fold change of miRNA-375 levels of the various tumor samples (T) with respect to the non-tumorous surrounding liver tissue (S), determined by qRT-PCR analysis. GAPDH was used as an endogenous normalizer. Results are expressed as means ± SE of three RT-PCRs per sample.

4.4.1 - Hippo and Wnt pathway cooperation in cancer cells arising in hyperplastic livers

Recent reports have suggested that the Hippo signaling pathway networks with other well-established pathways, including the Wnt signaling pathway (Sudol and Harvey, 2010). Wnts consist of a big family of secreted proteins which act as morphogens to control cell fate, differentiation, and proliferation. Wnts bind to cell-surface Frizzled (FRZ) and low-density lipoprotein receptor-related protein (LRP) receptors and thereby stimulate diverse biological responses (Clevers, 2006; Nusse, 2005). At the core of the canonical Wnt pathway is the transcriptional regulator β-catenin. In the absence of Wnt stimulation, β-catenin levels are kept low by proteasome-mediated degradation (Aberle *et al.*, 1997). Activation of Wnt signaling induces the hyperphosphorylation of Dishevelled (DVL), and this, via a poorly understood mechanism, ultimately leads to a rise in cytoplasmic β-catenin levels, which enables its nuclear translocation and, successively, to the activation of β-catenin target genes (Clevers, 2006; Nusse, 2005).

Varelas *et al.* (2010), recently indicated that loss of Hippo pathway activity leads to increased nuclear TAZ (the other transcriptional coactivator which, together with YAP, is antagonized by the Hippo kinase cascade) and reduces cytoplasmic TAZ-DVL binding, hence, causing an increase in Wnt-stimulated DVL phosphorylation, β-catenin nuclear accumulation, and, ultimately, induction of Wnt target genes (**Fig. 31**).

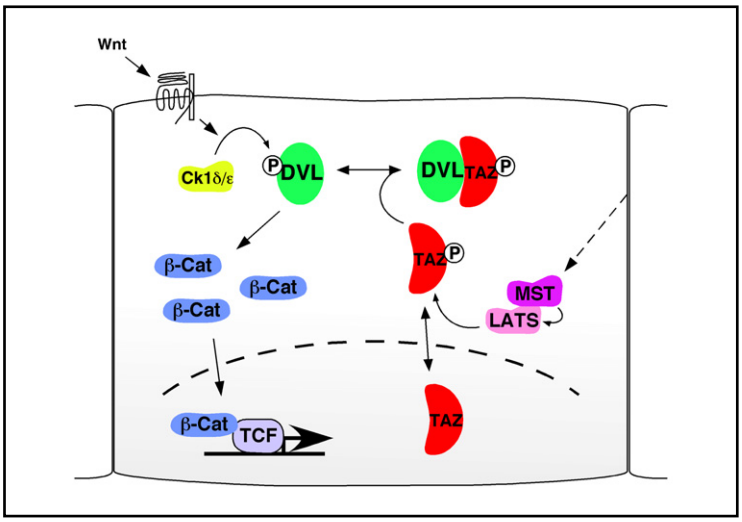

Fig. 31 Hippo kinase cascade-mediated regulation of Wnt signaling pathway via TAZ (Varelas *et al.*, 2010).

Since in the present study it was demonstrated that cancer cells were still able to proliferate in response to repeated stimulus of TCPOBOP, supporting the loss of activity of the Hippo tumor-suppressor pathway, levels of β-catenin in total protein extracts of hepatic tumors from the 28-week time point of the DENA + TCPOBOP group, were analyzed by Western Blot. Densitometric analysis showed that in all (21/21) tumor samples, levels of β-catenin almost increased by a mean fold of three, reflecting roughly the same trend as that for YAP protein (**Fig. 32**). Knowing that TAZ is recognized as an evolutionarily conserved paralog of YAP, with various similarities, and probably subserve separate but perhaps overlapping functions (Kanai *et al.*, 2000), it can be assumed that the behavior of YAP, in this case, is identical to that of TAZ. Hence, deducing that Hippo signaling pathway inactivation leads to nuclear translocation of YAP, which, after a series of signal transduction cascades, culminates with β-catenin nuclear accumulation that successively induces Wnt target genes.

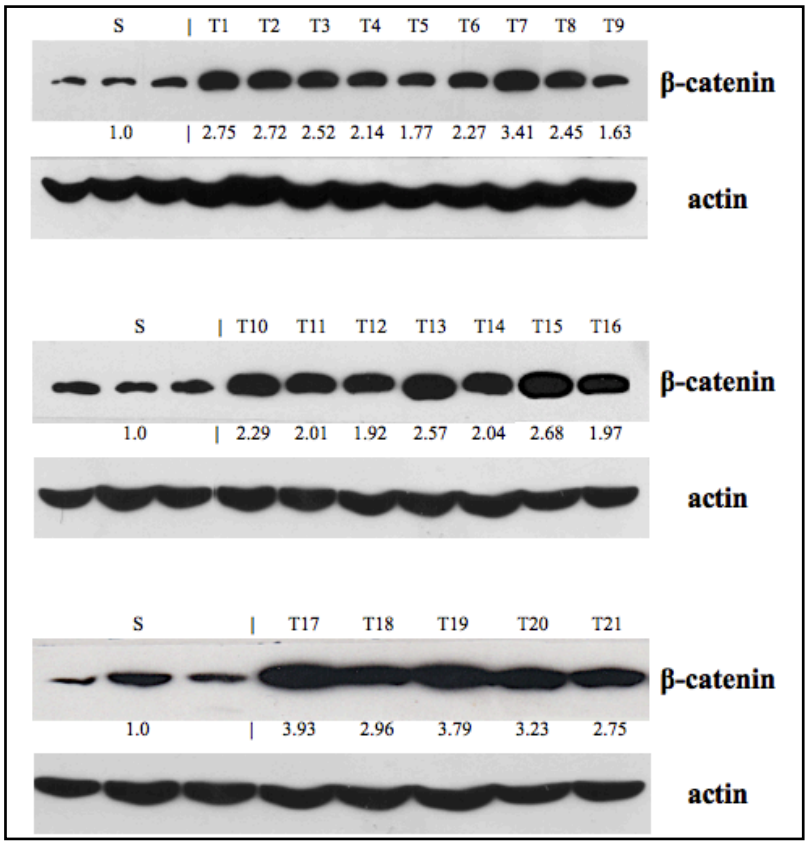

Fig. 32 Levels of β-catenin in total protein extracts of the various tumor samples (T) with respect to the non-tumorous surrounding liver tissue (S), determined by Western Blot analysis. Actin was used as a loading control. Each lane represents a single sample. Relative expression values determined by densitometric analysis are reported under each band.

Cadoret *et al.* (2002), indicated that glutamine synthetase (GS), together with two other genes, all belonging to the glutamine metabolism pathway, is a transcriptional target of β-catenin. Successive studies demonstrated that the same target gene was strongly upregulated in tumors exhibiting *Ctnnb1* mutations, whereas tumors lacking *Ctnnb1* mutations were negative for GS expression (Loeppen *et al.*, 2002).

On these bases, in order to evaluate the transcriptional activation of *β-catenin* in DENA + TCPOBOP-induced tumors, GS immunohistochemistry was carried out, in the same samples analyzed before for β-catenin protein expression. In the normal surrounding liver tissue, GS staining was circumscribed to few hepatocytes around the terminal central veins, a staining pattern that was first described by Gebhardt and Mecke (1983). On the contrary, the majority of tumors in these liver sections were GS-positive, with most neoplastic lesions showing a relatively homogeneous GS-staining pattern, although a heterogeneous expression of GS was also noticed in a small number of tumors (**Fig. 33**).

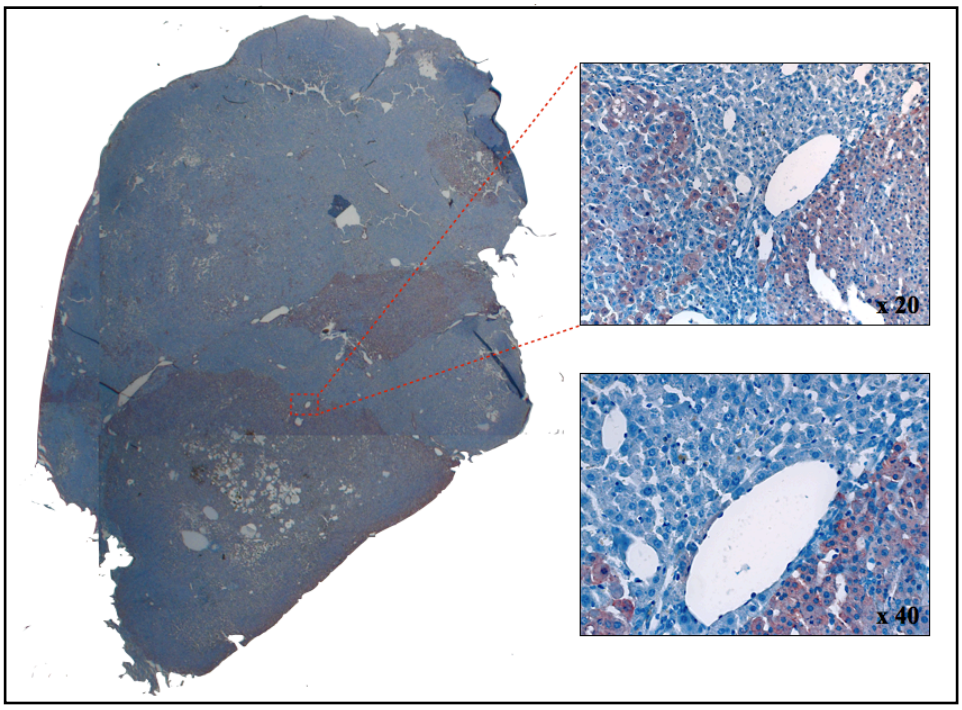

Fig. 33 Left Panel: Overview of a liver section from a mouse belonging to the 28-week time point of the DENA + TCPOBOP group stained immunohistochemically for GS. Right Panels: Selected area of one of the tumors at higher magnifications (originally x 20 and x 40).

A more recent study, reported that GS-positive hepatic tumors also exhibited increased expression of several CYP isoforms, as a consequence of direct or indirect transcriptional activation by β-catenin. Among these genes, Cyp2e1 is of major interest, being found, together with Cyp1a, to express more pronounced staining when compared to all other isoforms (Loeppen *et al.*, 2005).

When the same liver sections were stained for Cyp2e1, identical results to those obtained with GS staining were observed. In other words, the largest part of the neoplastic lesions, unlike the non-tumorous surrounding tissue, stained positively for Cyp2e1 (**Fig. 34**).

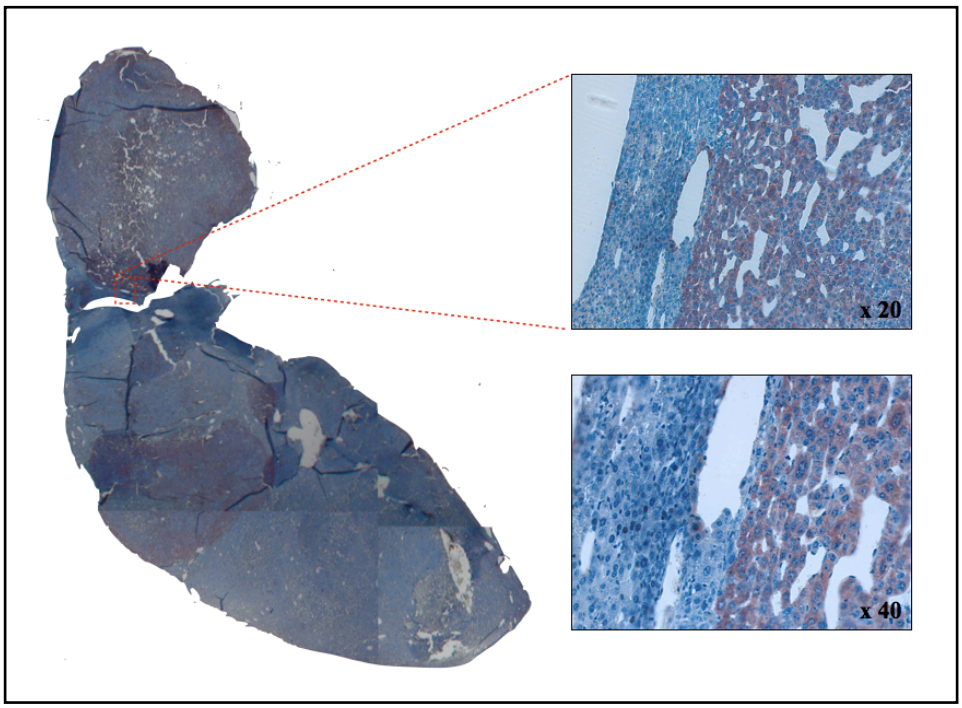

Fig. 34 Left Panel: Overview of a liver section from a mouse belonging to the 28-week time point of the DENA + TCPOBOP group stained immunohistochemically for Cyp2e1. Right Panels: Selected area of one of the tumors at higher magnifications (originally x 20 and x 40).

Since Loeppen *et al.* in 2002 and 2005, showed that the GS and Cyp2e1 target genes were strongly upregulated in tumors exhibiting *β-catenin* mutations, DENA + TCPOBOP-induced tumors, were screened for eventual alterations of *Ctnnb1*, in the same samples analyzed before for the transcriptional activation of *β-catenin*.

Primers originally designed by de La Coste *et al.* (1998) and Devereux *et al.* (1999), and later modified by Aydinlik *et al.* (2001), utilized to extent the entire region of the gene (1473 bp fragment) previously shown to contain deletions of varying length in liver tumors, did not detect any deletions. On the other hand, primers designed by Hailfinger *et al.* (2006) for point mutations at the known hotspots in exon 3 (248 bp fragment), showed a prevalence of almost 75% (16/21). Mutations in *Ctnnb1* were localized at codons 32, 33, 35, 37 and 41 (first described by Devereux *et al.*, 1999; Aydinlik *et al.*, 2001; Strathmann *et al.*, 2006; de La Coste *et al.*, 1998) (**Table 5**), all of which affect, either directly or indirectly, glycogen synthase kinase 3β (GSK3β)-mediated phosphorylation. The two types of base substitutions observed were transitions from A or T to G or C, respectively (**Fig. 35**).

Knowing that phosphorylation of β-catenin by GSK3β leads ultimately to β-catenin degradation (Willert and Nusse, 1998; Morin, 1999), hence such mutations augment β-catenin stability which cause a further increase in cytoplasmic β-catenin levels, potentiating the effect of the previously described YAP-mediated process in hepatic tumors.

	β-catenin* Mutations** ***(wildtype sequences of affected codons in parentheses)				
Codon	32 (GAT)	33 (TCT)	35 (ATC)	37 (TCT)	41 (ACC)
Mutated Sequence	G**G**T	**C**CT/**G**CT	A**G**C	**C**CT	**G**CC
Number of Tumors	2	3/1	6	2	1
Amino Acid Change	Asp → Gly	Ser → Pro/Ala	Ile → Ser	Ser → Pro	Thr → Ala

Table 5 Spectrum of single base substitutions and resulting amino acid changes in liver tumors of mice belonging to the 28-week time point of the DENA + TCPOBOP group.

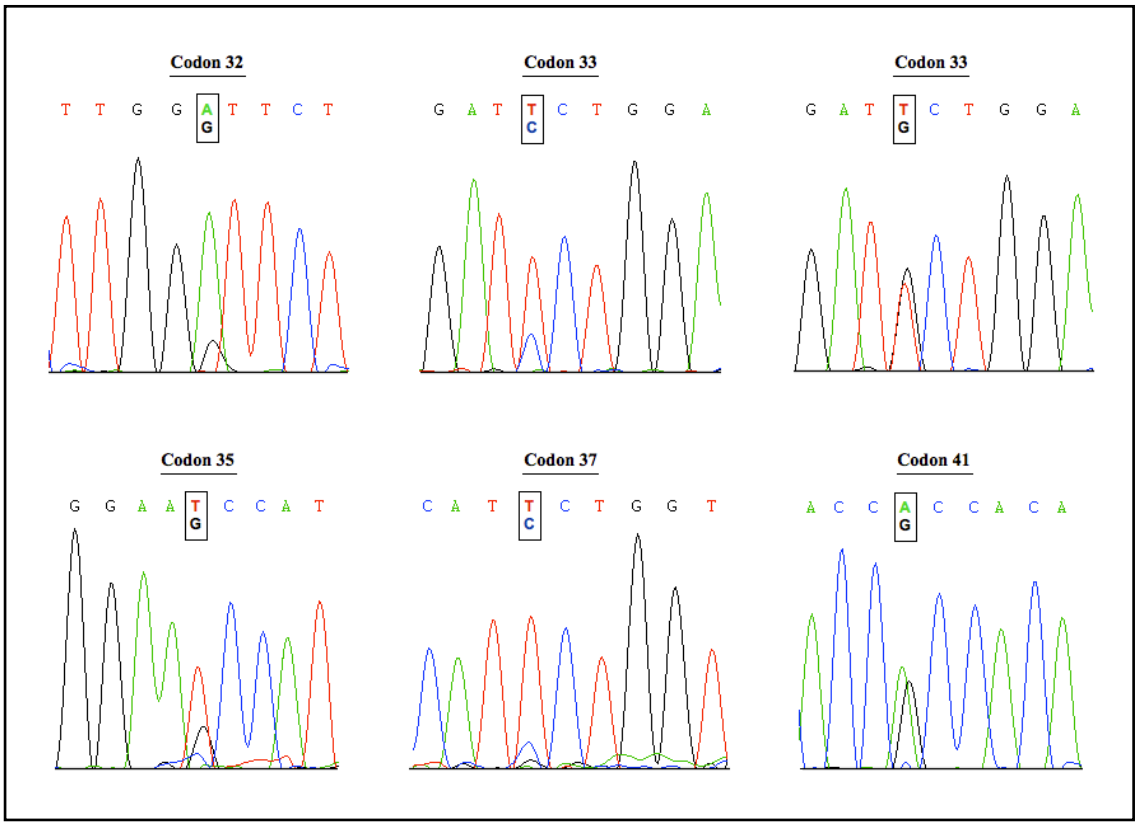

Fig. 35 Sequence analysis of the various point mutations in the different codons within the *β-catenin* gene in liver tumors of mice belonging to the 28-week time point of the DENA + TCPOBOP group.

Aydinlik *et al.* (2001) demonstrated that rodent liver tumors obtained with a single treatment of DENA followed by subsequent chronic administration of phenobarbital, according to a classical initiation-promotion experimental protocol, harbored neoplastic lesions that predominated in *Ctnnb1* mutations and lacked *Hras1* mutations. On these bases, since DENA + TCPOBOP-induced tumors showed a high prevalence of *β-catenin* mutations, a mutation analysis for *Ha-ras* was carried out.

The sense primer, used for the first time by Buchmann *et al.* (1991), and antisense primer, originally designed by Brown *et al.* (1990) and later used together by Jaworski *et al.* (2005), for single base substitutions in codon 61 within coding exon 2 (166 bp fragment), did not detect any mutations. This was later confirmed by analysis of appropriate RFLPs (as described by Buchmann *et al.*, 1991 and Bauer-Hofmann *et al.*, 1992) (**Fig. 36**).

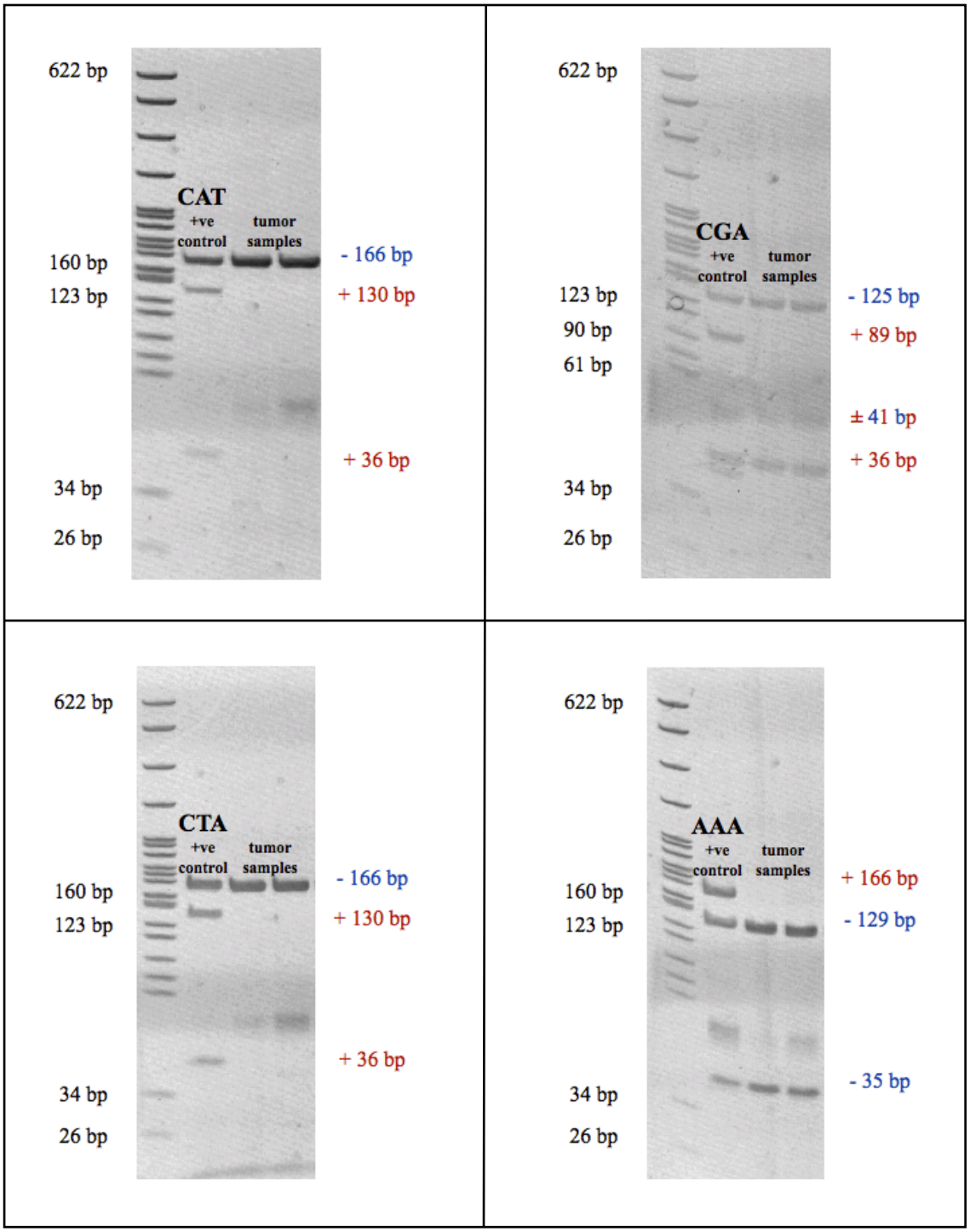

Fig. 36 RFLP analysis of the various single base substitutions in codon 61 within *Ha-ras* gene in hepatic tumors of mice belonging to the 28-week time point of the DENA + TCPOBOP group. *Hras1* mutations generate new restriction enzyme recognition sites which can be detected by *BspHI*, *TaqI* and *XbaI* enzymes (for mutated sequences CAT, CGA and CTA respectively), whereas the mutated sequence AAA leads to the loss of the *Hpy188III* enzyme recognition site. Mutation-specific fragments are marked by a red colored positive sign next to the size of the fragment.

These results confirm that tumors initiated with a single dose of DENA and promoted by chronic exposure to a CAR agonist, such as TCPOBOP, present majorly *Ctnnb1* mutations and lack *Hras1* mutations.

Chapter 5

Conclusions

In conclusion, data obtained from this study clearly demonstrates that in direct hyperplasia, achieved by xenobiotic administration, the Hippo pathway acts as a key regulator depending strictly on the organ size. Particularly, the liver becomes rapidly refractory to the mitogenic effect of TCPOBOP following repeated administration. Remarkably, activation of the Hippo growth-suppressive pathway, thus YAP inactivation, being responsible for the homeostatic mechanism triggered to prevent an abnormal liver size.

Moreover, data emerged from this study showed evidently that the same xenobiotic, which acts as non-genotoxic liver carcinogen following chronic administration, allow 'initiated' hepatocytes to selectively 'escape' from the previously described organ constraint, leading ultimately to HCC. Specifically, in TCPOBOP-dependent carcinogenesis, DENA-induced mutations are able to continue proliferating in spite of repeated administration of the mitogen, thus favoring their clonal expansion. Strikingly, dysregulation of the Hippo tumor-suppressive pathway, hence normal YAP activity interruption contributes to uncontrolled hepatocyte proliferation, leading ultimately to such tumor growth.

Furthermore, data obtained from this study indicated that Hippo signaling pathway inactivation in such tumors leads to nuclear translocation of YAP, which, after a series of signal transduction cascades, culminates with β-catenin nuclear accumulation that successively induces Wnt target genes. In addition, mutations augment β-catenin stability which cause a further increase in cytoplasmic β-catenin levels, potentiating the effect of the previously described YAP-mediated process in hepatic tumors.

References

Aberle, H., Bauer, A., Stappert, J., Kispert, A., Kemler, R. (1997) β-catenin is a target for the ubiquitin-proteasome pathway. *EMBO J*, **16(13)**, 3797-3804.

Ambros, V. (2004) The functions of animal microRNAs. *Nature*, **431(7006)**, 350-355.

Ames, B.N., Gold, L.S. (1990) Too many rodent carcinogens: mitogenesis increases mutagenesis. *Science*, **249(4972)**, 970-971.

Aranda, A., Pascual, A. (2001) Nuclear hormone receptors and gene expression. *Physiol Rev*, **81(3)**, 1269-1304.

Aydinlik, H., Nguyen, T.D., Moennikes, O., Buchmann, A., Schwarz, M. (2001) Selective pressure during tumor promotion by phenobarbital leads to clonal outgrowth of β-catenin-mutated mouse liver tumors. *Oncogene*, **20(53)**, 7812-7816.

Badouel, C., Gardano, L., Amin, N., Garg, A., Rosenfeld, R., Le Bihan, T., McNeill, H. (2009) The FERM-domain protein Expanded regulates Hippo pathway activity via direct interactions with the transcriptional activator Yorkie. *Dev Cell*, **16(3)**, 411-420.

Bartel, D.P. (2004) MicroRNAs: genomics, biogenesis, mechanism, and function. *Cell*, **116(2)**, 281-297.

Basu, S., Totty, N.F., Irwin, M.S., Sudol, M., Downward, J. (2003) Akt phosphorylates the Yes-associated protein, YAP, to induce interaction with 14-3-3 and attenuation of p73-mediated apoptosis. *Mol Cell*, **11(1)**, 11-23.

Bauer-Hofmann, R., Klimek, F., Buchmann, A., Müller, O., Bannasch, P., Schwarz, M. (1992) Role of mutations at codon 61 of the c-Ha-ras gene during diethylnitrosamine-induced hepatocarcinogenesis in C3H/He mice. *Mol Carcinog*, **6(1)**, 60-67.

Braconi, C., Patel, T. (2008) MicroRNA expression profiling: a molecular tool for defining the phenotype of hepatocellular tumors. *Hepatology*, **47(6)**,1807-1809.

Bradford, M. (1976) A rapid and sensitive method for the quantitation of microgram quantities of protein using the principle of protein-dye binding. *Anal Biochem*, **72**, 248-254.

Brigstock, D.R. (1999) The connective tissue growth factor/cysteine-rich 61/ nephroblastoma overexpressed (CCN) Family. *Endocr Rev*, **20(2)**,189-206.

Brown, K., Buchmann, A., Balmain, A. (1990) Carcinogen-induced mutations in the mouse c-Ha-ras gene provide evidence of multiple pathways for tumor progression. *Proc Natl Acad Sci U S A*, **87(2)**, 538-542.

Buchmann, A., Bauer-Hofmann, R., Mahr, J., Drinkwater, N.R., Luz, A., Schwarz, M. (1991) Mutational activation of the c-Ha-ras gene in liver tumors of different rodent strains: correlation with susceptibility to hepatocarcinogenesis. *Proc Natl Acad Sci U S A*, **88(3)**, 911-915.

Buttitta, L.A., Edgar, B.A. (2007) How size is controlled: from Hippos to Yorkies. *Nat Cell Biol*, **9(11)**, 1225-1227.

Cadoret, A., Ovejero, C., Terris, B., Souil, E., Lévy, L., Lamers, W.H., Kitajewski, J., Kahn, A., Perret, C. (2002) New targets of β-catenin signaling in the liver are involved in glutamine metabolism. *Oncogene*, **21(54)**, 8293-8301.

Callus, B.A., Verhagen, A.M., Vaux, D.L. (2006) Association of mammalian sterile twenty kinases, Mst1 and Mst2, with hSalvador via C-terminal coiled-coil domains, leads to its stabilization and phosphorylation. *FEBS J*, **273(18)**, 4264-4276.

Camargo, F.D., Gokhale, S., Johnnidis, J.B., Fu, D., Bell, G.W., Jaenisch, R., Brummelkamp, T.R. (2007) YAP1 increases organ size and expands undifferentiated progenitor cells. *Curr Biol*, **17(23)**, 2054-2060.

Chan, E.H., Nousiainen, M., Chalamalasetty, R.B., Schfer, A., Nigg, E.A., Silljé, H.H. (2005) The Ste20-like kinase Mst2 activates the human large tumor suppressor kinase Lats1. *Oncogene*, **24(12)**, 2076-2086.

Chan, S.W., Lim, C.J., Loo, L.S., Chong, Y.F., Huang, C., Hong, W. (2009) TEADs mediate nuclear retention of TAZ to promote oncogenic transformation. *J Biol Chem*, **284(21)**, 14347-14358.

Chen, L., Chan, S.W., Zhang, X., Walsh, M., Lim, C.J., Hong, W., Song, H. (2010) Structural basis of YAP recognition by TEAD4 in the hippo pathway. *Genes Dev*, **24(3)**, 290-300.

Chow, A., Hao, Y., Yang, X. (2010) Molecular characterization of human homologs of yeast MOB1. *Int J Cancer*, **126(9)**, 2079-2089.

Clevers, H. (2006) Wnt/β-catenin signaling in development and disease. *Cell*, **127(3)**, 469-480.

Columbano, A., Ledda-Columbano, G.M. (2003) Mitogenesis by ligands of nuclear receptors: an attractive model for the study of the molecular mechanisms implicated in liver growth. *Cell Death Differ*, **10(S1)**, S19-21.

Columbano, A., Shinozuka, H. (1996) Liver regeneration versus direct hyperplasia. *FASEB J*, **10(10)**, 1118-1128.

Conlon, I., Raff, M. (1999) Size control in animal development. *Cell*, **96(2)**, 235-244.

Cook, M.J. (1965) The Anatomy of the Laboratory Mouse [online]. London: Academic Press, p 58. Available from: http://www.informatics.jax.org//cookbook/ [Accessed 23 January 2008]

Cooper, W.N., Hesson, L.B., Matallanas, D., Dallol, A., von Kriegsheim, A., Ward, R., Kolch, W., Latif, F. (2009) RASSF2 associates with and stabilizes the proapoptotic kinase MST2. *Oncogene*, **28(33)**, 2988-2998.

de La Coste, A., Romagnolo, B., Billuart, P., Renard, C.A., Buendia, M.A., Soubrane, O., Fabre, M., Chelly, J., Beldjord, C., Kahn, A., Perret, C. (1998) Somatic mutations of the β-catenin gene are frequent in mouse and human hepatocellular carcinomas. *Proc Natl Acad Sci U S A*, **95(15)**, 8847-8851.

Devereux, T.R., Anna, C.H., Foley, J.F., White, C.M., Sills, R.C., Barrett, J.C. (1999) Mutation of β-catenin is an early event in chemically induced mouse hepatocellular carcinogenesis. *Oncogene*, **18(33)**, 4726-4733.

Dilworth, F.J., Chambon, P. (2001) Nuclear receptors coordinate the activities of chromatin remodeling complexes and coactivators to facilitate initiation of transcription. *Oncogene*, **20(24)**, 3047-3054.

Diwan, B.A., Rice, J.M., Ohshima, M., Ward, J.M. (1986) Interstrain differences in susceptibility to liver carcinogenesis initiated by N-nitrosodiethylamine and its promotion by phenobarbital in C57BL/6NCr, C3H/HeNCrMTV- and DBA/2NCr mice. *Carcinogenesis*, **7(2)**, 215-220.

Diwan, B.A., Rice, J.M., Nims, R.W., Lubet, R.A., Hu, H., Ward, J.M. (1988) P-450 enzyme induction by 5-ethyl-5-phenylhydantoin and 5,5-diethylhydantoin, analogs of the barbiturate tumor promoters phenobarbital and barbital, and promotion of liver and thyroid carcinogenesis initiated by N-nitrosodiethylamine in rats. *Cancer Res*, **48(9)**, 2492-2497.

Diwan, B.A., Lubet, R.A., Ward, J.M., Hrabie, J.A., Rice, J.M. (1992) Tumor-promoting and hepatocarcinogenic effects of l,4-bis[2-(3,5-dichloropyridyloxy)]benzene (TCPOBOP) in DBA/2NCr and C57BL/6NCr mice and an apparent promoting effect on nasal cavity tumors but not on hepatocellular tumors in F344/NCr rats initiated with N-nitrosodiethylamine. *Carcinogenesis*, **13(10)**, 1893-1901.

Dong, J., Feldmann, G., Huang, J., Wu, S., Zhang, N., Comerford, S.A., Gayyed, M.F., Anders, R.A., Maitra, A., Pan, D. (2007) Elucidation of a universal size-control mechanism in *Drosophila* and mammals. *Cell*, **130(6)**, 1120-1133.

Dragani, T.A., Manenti, G., Galliani, G., Della Porta, G. (1985) Promoting effects of l, 4-bis[2-(3,5-dichloropyridyloxy)]benzene in mouse hepatocarcinogenesis. *Carcinogenesis*, **6(2)**, 225-228.

Dragani, T.A., Manenti, G., Della Porta, G. (1987) Genetic susceptibility to murine hepatocarcinogenesis is associated with high growth rate of NDEA-initiated hepatocytes. *J Cancer Res Clin Oncol*, **113(3)**, 223-229.

Edgar, B.A. (2006) From cell structure to transcription: Hippo forges a new path. *Cell*, **124(2)**, 267-273.

Forman, B.M., Tzameli, I., Choi, H.S., Chen, J., Simha, D., Seol, W., Evans, R.M., Moore, D.D. (1998) Androstane metabolites bind to and deactivate the nuclear receptor CAR-β. *Nature*, **395(6702)**, 612-615.

Fornari, F., Milazzo, M., Chieco, P., Negrini, M., Calin, G.A., Grazi, G.L., Pollutri, D., Croce, C.M., Bolondi, L., Gramantieri. L. (2010) MiR-199a-3p regulates mTOR and c-Met to influence the doxorubicin sensitivity of human hepatocarcinoma cells. *Cancer Res*, **70(12)**, 5184-5193.

Gebhardt, R., Mecke, D. (1983) Heterogeneous distribution of glutamine synthetase among rat liver parenchymal cells in situ and in primary culture. *EMBO J*, **2(4)**, 567-570.

Germain, P., Staels, B., Dacquet, C., Spedding, M., Laudet, V. (2006) Overview of nomenclature of nuclear receptors. *Pharmacol Rev*, **58(4)**, 685-704.

Goulev, Y., Fauny, J.D., Gonzalez-Marti, B., Flagiello, D., Silber, J., Zider, A. (2008) SCALLOPED interacts with YORKIE, the nuclear effector of the Hippo tumor-suppressor pathway in Drosophila. *Curr Biol*, **18(6)**, 435-441.

Hailfinger, S., Jaworski, M., Braeuning, A., Buchmann, A., Schwarz, M. (2006) Zonal gene expression in murine liver: lessons from tumors. *Hepatology*, **43(3)**, 407-414.

Hao, Y., Chun, A., Cheung, K., Rashidi, B., Yang, X. (2008) Tumor suppressor LATS1 is a negative regulator of oncogene YAP. *J Biol Chem*, **283(9)**, 5496-5509.

Harvey, K.F., Pfleger, C.M., Hariharan, I.K. (2003) The Drosophila Mst ortholog, hippo, restricts growth and cell proliferation and promotes apoptosis. *Cell*, **114(4)**, 457-467.

Hergovich, A., Schmitz, D., Hemmings, B.A. (2006) The human tumour suppressor LATS1 is activated by human MOB1 at the membrane. *Biochem Biophys Res Commun*, **345(1)**, 50-58.

Higgins, G.M., Anderson, R.M. (1931) Experimental pathology of the liver. Restoration of the liver of the white rat following partial surgical removal. *Arch Pathol*, **12(1)**, 186-202.

Hirabayashi, S., Nakagawa, K., Sumita, K., Hidaka, S., Kawai, T., Ikeda, M., Kawata, A., Ohno, K., Hata, Y. (2008) Threonine 74 of MOB1 is a putative key phosphorylation site by MST2 to form the scaffold to activate nuclear Dbf2-related kinase 1. *Oncogene*, **27(31)**, 4281-4292.

Hisaoka, M., Tanaka, A., Hashimoto, H. (2002) Molecular alterations of h-warts/LATS1 tumor suppressor in human soft tissue sarcoma. *Lab Invest*, **82(10)**, 1427-1435.

Ho, L.L., Wei, X., Shimizu, T., Lai, Z.C. (2009) Mob as tumor suppressor is activated at the cell membrane to control tissue growth and organ size in Drosophila. *Dev Biol*, **337 (2)**, 274-283.

Honkakoski, P., Moore, R., Washburn, K.A., Negishi, M. (1998a) Activation by diverse xenochemicals of the 51-base pair phenobarbital-responsive enhancer module in the CYP2B10 gene. *Mol Pharmacol*, **53(4)**, 597-601.

Honkakoski, P., Zelko, I., Sueyoshi, T., Negishi, M. (1998b) The nuclear orphan receptor CAR-retinoid X receptor heterodimer activates the phenobarbital-responsive enhancer module of the CYP2B gene. *Mol Cell Biol*, **18(10)**, 5652-5658.

Honkakoski, P., Sueyoshi, T., Negishi, M. (2003) Drug-activated nuclear receptors CAR and PXR. *Ann Med*, **35(3)**, 172-182.

Huang, J., Wu, S., Barrera, J., Matthews, K., Pan, D. (2005) The Hippo signaling pathway coordinately regulates cell proliferation and apoptosis by inactivating Yorkie, the Drosophila Homolog of YAP. *Cell*, **122(3)**, 421-434.

Inui, M., Martello, G., Piccolo, S. (2010) MicroRNA control of signal transduction. *Nat Rev Mol Cell Biol*,**11(4)**, 252-263.

Iorio, M.V., Croce, C.M. (2009) MicroRNAs in cancer: small molecules with a huge impact. *J Clin Oncol*, **27(34)**, 5848-5856.

Jaworski, M., Buchmann, A., Bauer, P., Riess, O., Schwarz, M. (2005) B-raf and Ha-ras mutations in chemically induced mouse liver tumors. *Oncogene*, **24(7)**, 1290-5.

Jia, J., Zhang, W., Wang, B., Trinko, R., Jiang, J. (2003) The Drosophila Ste20 family kinase dMST functions as a tumor suppressor by restricting cell proliferation and promoting apoptosis. *Genes Dev*, **17(20)**, 2514-2519.

Jiang, Z., Li, X., Hu, J., Zhou, W., Jiang, Y., Li, G., Lu, D. (2006) Promoter hypermethylation-mediated down-regulation of LATS1 and LATS2 in human astrocytoma. *Neurosci Res*, **56(4)**, 450-458.

Justice, R.W., Zilian, O., Woods, D.F., Noll, M., Bryant, P.J. (1995) The Drosophila tumor suppressor gene warts encodes a homolog of human myotonic dystrophy kinase and is required for the control of cell shape and proliferation. *Genes Dev*, **9(5)**, 534-546.

Kanai, F., Marignani, P.A., Sarbassova, D., Yagi, R., Hall, R.A., Donowitz, M., Hisaminato, A., Fujiwara, T., Ito, Y., Cantley, L.C., Yaffe, M.B. (2000) TAZ: a novel transcriptional co-activator regulated by interactions with 14-3-3 and PDZ domain proteins. *EMBO J*, **19(24)**, 6778-6791.

Kango-Singh, M., Nolo, R., Tao, C., Verstreken, P., Hiesinger, P.R., Bellen, H.J., Halder, G. (2002) Shar-pei mediates cell proliferation arrest during imaginal disc growth in Drosophila. *Development*, **129(24)**, 5719-5730.

Kawamoto, T., Sueyoshi, T., Zelko, I., Moore, R., Washburn, K., Negishi, M. (1999) Phenobarbital-responsive nuclear translocation of the receptor CAR in induction of the CYP2B gene. *Mol Cell Biol*, **19(9)**, 6318-6322.

Kelly, M., Womack, J., Safe, S. (1990) Effects of cytochrome P-450 monooxygenase inducers on mouse hepatic microsomal metabolism of testosterone and alkoxyresorufins. *Biochem Pharmacol*, **39(12)**, 1991-2004.

Khokhlatchev, A., Rabizadeh, S., Xavier, R., Nedwidek, M., Chen, T., Zhang, X.F., Seed, B., Avruch, J. (2002) Identification of a novel Ras-regulated proapoptotic pathway. *Curr Biol*, **12(4)**, 253-265.

Kliewer, S.A., Umesono, K., Mangelsdorf, D.J., Evans, R.M. (1992) Retinoid X receptor interacts with nuclear receptors in retinoic acid, thyroid hormone and vitamin D3 signaling. *Nature*, **355(6359)**, 446-449.

Kobayashi, K., Sueyoshi, T., Inoue, K., Moore, R., Negishi, M. (2003) Cytoplasmic accumulation of the nuclear receptor CAR by a tetratricopeptide repeat protein in HepG2 cells. *Mol Pharmacol*, **64(5)**, 1069-1075.

Komuro, A., Nagai, M., Navin, N.E., Sudol, M. (2003) WW domain-containing protein YAP associates with ErbB-4 and acts as a co-transcriptional activator for the carboxyl-terminal fragment of ErbB-4 that translocates to the nucleus. *J Biol Chem*, **278(35)**, 33334-33341.

Ladeiro, Y., Couchy, G., Balabaud, C., Bioulac-Sage, P., Pelletier, L., Rebouissou, S., Zucman-Rossi, J. (2008) MicroRNA profiling in hepatocellular tumors is associated with clinical features and oncogene/tumor supressor gene mutations. *Hepatology*, **47(6)**, 1955-1963.

Lai, Z.C., Wei, X., Shimizu, T., Ramos, E., Rohrbaugh, M., Nikolaidis, N., Ho, L.L., Li, Y. (2005) Control of cell proliferation and apoptosis by mob as tumor suppressor, mats. *Cell*, **120(5)**, 675-685.

Ledda-Columbano, G.M., Pibiri, M., Loi, R., Perra, A., Shinozuka, H., Columbano, A. (2000) Early increase in cyclin-D1 expression and accelerated entry of mouse hepatocytes into S phase after administration of the mitogen 1,4-Bis[2-(3,5-Dichloropyridyloxy)] benzene. *Am J Pathol*, **156(1)**, 91-97.

Ledda-Columbano, G.M., Pibiri, M., Concas, D., Molotzu, F., Simbula, G., Cossu, C., Columbano, A. (2003) Sex difference in the proliferative response of mouse hepatocytes to treatment with the CAR ligand, TCPOBOP. *Carcinogenesis*, **24(6)**, 1059-1065.

Ledda-Columbano, G.M., Pibiri, M., Cossu, C., Molotzu, F., Locker, J., Columbano, A. (2004) Aging does not reduce the hepatocyte proliferative response of mice to the primary mitogen TCPOBOP. *Hepatology*, **40(4)**, 981-988.

Lee, J.H., Kim, T.S., Yang, T.H., Koo, B.K., Oh, S.P., Lee, K.P., Oh, H.J., Lee, S.H., Kong, Y.Y., Kim, J.M., Lim, D.S. (2008) A crucial role of WW45 in developing epithelial tissues in the mouse. *Embo J*, **27(8)**, 1231-1242.

Lei, Q.Y., Zhang, H., Zhao, B., Zha, Z.Y., Bai, F., Pei, X.H., Zhao, S., Xiong, Y., Guan, K.L. (2008) TAZ promotes cell proliferation and epithelial-mesenchymal transition and is inhibited by the hippo pathway. *Mol Cell Biol*, **28(7)**, 2426-2436.

Li, Z., Zhao, B., Wang, P., Chen, F., Dong, Z., Yang, H., Guan, K.L., Xu, Y. (2010) Structural insights into the YAP and TEAD complex. *Genes Dev*, **24(3)**, 235-240.

Liu, A.M., Poon, R.T., Luk, J.M. (2010) MicroRNA-375 targets Hippo-signaling effector YAP in liver cancer and inhibits tumor properties. *Biochem Biophys Res Commun*, **394(3)**, 623-627.

Loeppen, S., Schneider, D., Gaunitz, F., Gebhardt, R., Kurek, R., Buchmann, A., Schwarz, M. (2002) Overexpression of glutamine synthetase is associated with β-catenin-mutations in mouse liver tumors during promotion of hepatocarcinogenesis by phenobarbital. *Cancer Res*, **62(20)**, 5685-5688.

Loeppen, S., Koehle, C., Buchmann, A., Schwarz, M. (2005) A β-catenin-dependent pathway regulates expression of cytochrome P450 isoforms in mouse liver tumors. *Carcinogenesis*, **26(1)**, 239-248.

Lu, L., Li, Y., Kim, S.M., Bossuyt, W., Liu, P., Qiu, Q., Wang, Y., Halder, G., Finegold, M.J., Lee, J.S., Johnson, R.L. (2010) Hippo signaling is a potent in vivo growth and tumor suppressor pathway in the mammalian liver. *Proc Natl Acad Sci U S A*, **107(4)**, 1437-1442.

Luo, X., Li, Z., Yan, Q., Li, X., Tao, D., Wang, J., Leng, Y., Gardner, K., Judge, S.I., Li, Q.Q., Hu, J., Gong, J. (2009) The human WW45 protein enhances MST1-mediated apoptosis in vivo. *Int J Mol Med*, **23(3)**, 357-362.

Maglich, J.M., Stoltz, C.M., Goodwin, B., Hawkins-Brown, D., Moore, J.T., Kliewer, S.A. (2002) Nuclear pregnane x receptor and constitutive androstane receptor regulate overlapping but distinct sets of genes involved in xenobiotic detoxification. *Mol Pharmacol*, **62(3)**, 638-646.

Manenti, G., Dragani, T.A., Della Porta, G. (1987) Effects of phenobarbital and 1,4-bis [2-(3,5-dichloropyridyloxy)]benzene on differentiated functions in mouse liver. *Chem Biol Interact*, **64(1-2)**, 83-92.

Mangelsdorf, D.J., Thummel, C., Beato, M., Herrlich, P., Schütz, G., Umesono, K., Blumberg, B., Kastner, P., Mark, M., Chambon, P., Evans, R.M. (1995) The nuclear receptor superfamily: the second decade. *Cell*, **83(6)**, 835-839.

Marsman, D.S., Cattley, R.C., Conway, J.G., Popp, J.A. (1988) Relationship of hepatic peroxisome proliferation and replicative DNA synthesis to the hepatocarcinogenicity of the peroxisome proliferators di(2-ethylhexyl)phthalate and [4-chloro-6-(2,3-xylidino)-2-pyrimidinylthio]acetic acid (Wy-14,643) in rats. *Cancer Res*, **48(23)**, 6739-6744.

McKenna, N.J., Xu, J., Nawaz, Z., Tsai, S.Y., Tsai, M.J., O'Malley, B.W. (1999) Nuclear receptor coactivators: multiple enzymes, multiple complexes, multiple functions. *J Steroid Biochem Mol Biol*, **69(1-6)**, 3-12.

McPherson, J.P., Tamblyn, L., Elia, A., Migon, E., Shehabeldin, A., Matysiak-Zablocki, E., Lemmers, B., Salmena, L., Hakem, A., Fish, J., Kassam, F., Squire, J., Bruneau, B.G., Hande, M.P., Hakem, R. (2004) Lats2/Kpm is required for embryonic development, proliferation control and genomic integrity. *EMBO J*, **23(18)**, 3677-3688.

Michalopoulos, G.K. (2007) Liver regeneration. *J Cell Physiol*, **213(2)**, 286-300.

Morin, P.J. β-catenin signaling and cancer. (1999) *BioEssays*, **21(12)**, 1021-1030.

Morinaga, N., Shitara, Y., Yanagita, Y., Koida, T., Kimura, M., Asao, T., Kimijima, I., Takenoshita, S., Hirota, T., Saya, H., Kuwano, H. (2000) Molecular analysis of the h-warts/LATS1 gene in human breast cancer. *Int J Oncol*, **17(6)**, 1125-1129.

Nolo, R., Morrison, C.M., Tao, C., Zhang, X., Halder, G. (2006) The bantam microRNA is a target of the hippo tumor-suppressor pathway. *Curr Biol*, **16(19)**, 1895-1904.

Nusse, R. (2005) Wnt signaling in disease and in development. *Cell Res*, **15(1)**, 28-32.

O'Neill, E., Rushworth, L., Baccarini, M., Kolch, W. (2004) Role of the kinase MST2 in suppression of apoptosis by the proto-oncogene product Raf-1. *Science*, **306(5705)**, 2267-2270.

O'Neill, E., Kolch, W. (2005) Taming the Hippo: Raf-1 controls apoptosis by suppressing MST2/Hippo. *Cell Cycle*, **4(3)**, 365-367.

Oh, H., Irvine, K.D. (2008) In vivo regulation of Yorkie phosphorylation and localization. *Development*, **135(6)**, 1081-1088.

Oh, H., Irvine, K.D. (2009) In vivo analysis of Yorkie phosphorylation sites. *Oncogene*, **28(17)**, 1916-1927.

Oh, H.J., Lee, K.K., Song, S.J., Jin, M.S., Song, M.S., Lee, J.H., Im, C.R., Lee, J.O., Yonehara, S., Lim, D.S. (2006) Role of the tumor suppressor RASSF1A in Mst1-mediated apoptosis. *Cancer Res*, **66(5)**, 2562-2569.

Oh, S., Lee, D., Kim, T., Kim, T.S., Oh, H.J., Hwang, C.Y., Kong, Y.Y., Kwon, K.S., Lim, D.S. (2009) Crucial role for Mst1 and Mst2 kinases in early embryonic development of the mouse. *Mol Cell Biol*, **29(23)**, 6309-6320.

Overholtzer, M., Zhang, J., Smolen, G.A., Muir, B., Li, W., Sgroi, D.C., Deng, C.X., Brugge, J.S., Haber, D.A. (2006) Transforming properties of YAP, a candidate oncogene on the chromosome 11q22 amplicon. *Proc Natl Acad Sci U S A*, **103(33)**, 12405-12410.

Pantalacci, S., Tapon, N., Léopold, P. (2003) The Salvador partner Hippo promotes apoptosis and cell-cycle exit in Drosophila. *Nat Cell Biol*, **5(10)**, 921-927.

Pines, J. (1995) Cyclins and cyclin-dependent kinases: a biochemical view. *Biochem J*, **308(3)**, 697-711.

Poland, A., Mak, I., Glover, E., Boatman, R.J., Ebetino, F.H., Kende, A.S. (1980) l,4-Bis [2-(3,5-dich]oropyridyloxy)]benzene, a potent phenobarbital-like inducer of microsomal monooxygenase activity. *Mol Pharmacol,* **18(3)**, 571-580.

Poland, A., Mak, I., Glover, E. (1981) Species differences in responsiveness to l,4-bis[2-(3,5-dichloropyridyloxy)]benzene) a potent phenobarbital-like inducer of microsomal monooxygenase activity. *Mol Pharmacol*, **20(2)**, 442-450.

Polesello, C., Huelsmann, S., Brown, N.H., Tapon, N. (2006) The Drosophila RASSF homolog antagonizes the hippo pathway. *Curr Biol*, **16(24)**, 2459-2465.

Praskova, M., Khoklatchev, A., Ortiz-Vega, S., Avruch, J. (2004) Regulation of the MST1 kinase by autophosphorylation, by the growth inhibitory proteins, RASSF1 and NORE1, and by Ras. *Biochem J*, **381(2)**, 453-462.

Praskova, M., Xia, F., Avruch, J. (2008) MOBKL1A/MOBKL1B phosphorylation by MST1 and MST2 inhibits cell proliferation. *Curr Biol*, **18(5)**, 311-321.

Raunio, H., Kojo, A., Juvonen, R., Honkakoski, P., Järvinen, P., Lang, M.A., Vähäkangas, K., Gelboin, H.V., Park, S.S., Pelkonen, O. (1988) Mouse hepatic cytochrome P-450 isozyme induction by 1,4-bis[2-(3,5-dichloropyridyloxy)]benzene, pyrazole, and phenobarbital. *Biochem Pharmacol*, **37(21)**, 4141-4147.

Ren, F., Zhang, L., Jiang, J. (2009) Hippo signaling regulates Yorkie nuclear localization and activity through 14–3–3 dependent and independent mechanisms. *Dev Biol*, **337(2)**, 303-312.

Romano, M., Esteve, A., Coccia, P., Masturzo, P., Galliani, G., Ghezzi, P., Salmona, M. (1986) Biochemical characterization of the hepatic effects in mice and rats of 1,4-bis[2-(3,5-dichloropyridyloxy)]benzene, a hepatic neoplasm promoter. *Toxicol Appl Pharmacol*, **83(2)**, 379-385.

Rosenfeld, J.M., Vargas, R. Jr., Xie, W., Evans, R.M. (2003) Genetic profiling defines the xenobiotic gene network controlled by the nuclear receptor pregnane X receptor. *Mol Endocrinol*, **17(7)**, 1268-1282.

Sawada, A., Kiyonari, H., Ukita, K., Nishioka, N., Imuta, Y., Sasaki, H. (2008) Redundant roles of Tead1 and Tead2 in notochord development and the regulation of cell proliferation and survival. *Mol Cell Biol*, **28(10)**, 3177-3189.

Shimizu, T., Ho, L.L., Lai, Z.C. (2008) The mob as tumor suppressor gene is essential for early development and regulates tissue growth in Drosophila. *Genetics*, **178(2)**, 957-965.

Smith, G., Henderson, C.J., Parker, M.G., White, R., Bars, R.G., Wolf, C.R. (1993) 1,4-Bis[2-(3,5-dichloropyridyloxy)]benzene, an extremely potent modulator of mouse hepatic cytochrome P-450 gene expression. *Biochem J*, **289(3)**, 807-813.

Song, H., Mak, K.K., Topol, L., Yun, K., Hu, J., Garrett, L., Chen, Y., Park, O., Chang, J., Simpson, R.M., Wang, C.Y., Gao, B., Jiang, J., Yang, Y. (2010) Mammalian Mst1 and Mst2 kinases play essential roles in organ size control and tumor suppression. *Proc Natl Acad Sci U S A*, **107(4)**, 1431-1436.

St John, M.A., Tao, W., Fei, X., Fukumoto, R., Carcangiu, M.L., Brownstein, D.G., Parlow, A.F., McGrath, J., Xu, T. (1999) Mice deficient of Lats1 develop soft-tissue sarcomas, ovarian tumours and pituitary dysfunction. *Nat Genet*, **21(2)**, 182-186.

Stegert, M.R., Hergovich, A., Tamaskovic, R., Bichsel, S.J., Hemmings, B.A. (2005) Regulation of NDR protein kinase by hydrophobic motif phosphorylation mediated by the mammalian Ste20-like kinase MST3. *Mol Cell Biol*, **25(24)**, 11019-11029.

Steinhardt, A.A., Gayyed, M.F., Klein, A.P., Dong, J., Maitra, A., Pan, D., Montgomery, E.A., Anders, R.A. (2008) Expression of Yes-associated protein in common solid tumors. *Hum Pathol*, **39(11)**, 1582-1589.

Strathmann, J., Schwarz, M., Tharappel, J.C., Glauert, H.P., Spear, B.T., Robertson, L.W., Appel, K.E., Buchmann, A. (2006) PCB 153, a non-dioxin-like tumor promoter, selects for β-catenin (*Catnb*)-mutated mouse liver tumors. *Toxicol Sci*, **93(1)**, 34-40.

Sudol, M., Bork, P., Einbond, A., Kastury, K., Druck, T., Negrini, M., Huebner, K., Lehman, D. (1995) Characterization of the mammalian YAP (Yes-associated protein) gene and its role in defining a novel protein module, the WW domain. *J Biol Chem*, **270 (24)**, 14733-14741.

Sudol, M., Harvey, K.F. (2010) Modularity in the Hippo signaling pathway. *Trends Biochem Sci*, **35(11)**, 627-633.

Sueyoshi, T., Kawamoto, T., Zelko, I., Honkakoski, P., Negishi, M. (1999) The repressed nuclear receptor CAR responds to phenobarbital in activating the human CYP2B6 gene. *J Biol Chem*, **274(10)**, 6043-6046.

Swales, K., Negishi, M. (2004) CAR, driving into the future. *Mol Endocrinol*, **18(7)**, 1589-1598.

Takahashi, Y., Miyoshi, Y., Takahata, C., Irahara, N., Taguchi, T., Tamaki, Y., Noguchi, S. (2005) Down-regulation of LATS1 and LATS2 mRNA expression by promoter hypermethylation and its association with biologically aggressive phenotype in human breast cancers. *Clin Cancer Res*, **11(4)**, 1380-1385.

Tapon, N., Harvey, K.F., Bell, D.W., Wahrer, D.C., Schiripo, T.A., Haber, D.A., Hariharan, I.K. (2002) Salvador promotes both cell cycle exit and apoptosis in Drosophila and is mutated in human cancer cell lines. *Cell*, **110(4)**, 467-478.

Thompson, B.J., Cohen, S.M. (2006) The Hippo pathway regulates the bantam microRNA to control cell proliferation and apoptosis in Drosophila. *Cell*, **126(4)**, 767-774.

Timchenko, N.A., Wilde, M., Nakanishi, M., Smith, J.R., Darlington, G.J. (1996) CCAAT/enhancer-binding protein alpha (C/EBP alpha) inhibits cell proliferation through the p21 (WAF-1/CIP-1/SDI-1) protein. *Genes & Dev*, **10(7)**, 804-815.

Tzameli, I., Pissios, P., Schuetz, E.G., Moore, D.D. (2000) The xenobiotic compound 1,4-bis[2-(3,5-dichloropyridyloxy)]benzene is an agonist ligand for the nuclear receptor CAR. *Mol Cell Biol*, **20(9)**, 2951-2958.

Udan, R.S., Kango-Singh, M., Nolo, R., Tao, C., Halder, G. (2003) Hippo promotes proliferation arrest and apoptosis in the Salvador/Warts pathway. *Nat Cell Biol*, **5(10)**, 914-920.

Ueda, A., Hamadeh, H.K., Webb, H.K., Yamamoto, Y., Sueyoshi, T., Afshari, C.A., Lehmann, J.M., Negishi, M. (2002) Diverse roles of the nuclear orphan receptor CAR in regulating hepatic genes in response to phenobarbital. *Mol Pharmacol*, **61(1)**, 1-6.

Varelas, X., Miller, B.W., Sopko, R., Song, S., Gregorieff, A., Fellouse, F.A., Sakuma, R., Pawson, T., Hunziker, W., McNeill, H., Wrana, J.L., Attisano, L. (2010) The Hippo pathway regulates Wnt/β-catenin signaling. *Dev Cell*, **18(4)**, 579-591.

Vassilev, A., Kaneko, K.J., Shu, H., Zhao, Y., DePamphilis, M.L. (2001) TEAD/TEF transcription factors utilize the activation domain of YAP65, a Src/Yes-associated protein localized in the cytoplasm. *Genes Dev*, **15(10)**, 1229-1241.

Vesselinovitch, S.D., Mihailovich, N., Rao, K.V. (1978) Morphology and metastatic nature of induced hepatic nodular lesions in C57BL x C3H F1 mice. *Cancer Res*, **38(7)**, 2003-2010.

Wei, P., Zhang, J., Egan-Hafley, M., Liang, S., Moore, D.D. (2000) The nuclear receptor CAR mediates specific xenobiotic induction of drug metabolism. *Nature*, **407(6806)**, 920-923.

Wei, P., Zhang, J., Dowhan, D.H., Han, Y., Moore, D.D. (2002) Specific and overlapping functions of the nuclear hormone receptors CAR and PXR in xenobiotic response. *Pharmacogenomics J*, **2(2)**, 117-126.

Wei, X., Shimizu, T., Lai, Z.C. (2007) Mob as tumor suppressor is activated by Hippo kinase for growth inhibition in Drosophila. *EMBO J*, **26(7)**, 1772-1781.

Willert, K., Nusse, R. (1998) β-catenin: a key mediator of Wnt signaling. *Curr Opin Genet Dev*, **8(1)**, 95-102.

Wu, S., Huang, J., Dong, J., Pan, D. (2003) Hippo encodes a Ste-20 family protein kinase that restricts cell proliferation and promotes apoptosis in conjunction with salvador and warts. *Cell*, **114(4)**, 445-456.

Wu, S., Liu, Y., Zheng, Y., Dong, J., Pan, D. (2008) The TEAD/TEF family protein Scalloped mediates transcriptional output of the Hippo growth-regulatory pathway. *Dev Cell*, **14(3)**, 388-398.

Xu, L., Glass, C.K., Rosenfeld, M.G. (1999) Coactivator and corepressor complexes in nuclear receptor function. *Curr Opin Genet Dev*, **9(2)**, 140-147.

Xu, T., Wang, W., Zhang, S., Stewart, R.A., Yu, W. (1995) Identifying tumor suppressors in genetic mosaics: the Drosophila lats gene encodes a putative protein kinase. *Development*, **121(4)**, 1053-1063.

Yabuta, N., Okada, N., Ito, A., Hosomi, T., Nishihara, S., Sasayama, Y., Fujimori, A., Okuzaki, D., Zhao, H., Ikawa, M., Okabe, M., Nojima, H. (2007) Lats2 is an essential mitotic regulator required for the coordination of cell division. *J Biol Chem*, **282(26)**, 19259-19271.

Yagi, R., Chen, L.F., Shigesada, K., Murakami, Y., Ito, Y. (1999) A WW domain-containing yes-associated protein (YAP) is a novel transcriptional co-activator. *EMBO J*, **18(9)**, 2551-2562.

Zelko, I., Sueyoshi, T., Kawamoto, T., Moore, R., Negishi, M. (2001) The peptide near the C terminus regulates receptor CAR nuclear translocation induced by xenochemicals in mouse liver. *Mol Cell Biol*, **21(8)**, 2838-2846.

Zender, L., Spector, M.S., Xue, W., Flemming, P., Cordon-Cardo, C., Silke, J., Fan, S.T., Luk, J.M., Wigler, M., Hannon, G.J., Mu, D., Lucito, R., Powers, S., Lowe, S.W. (2006) Identification and validation of oncogenes in liver cancer using an integrative oncogenomic approach. *Cell*, **125(7)**, 1253-1267.

Zhang, H., Liu, C.Y., Zha, Z.Y., Zhao, B., Yao, J., Zhao, S., Xiong, Y., Lei, Q.Y., Guan, K.L. (2009) TEAD transcription factors mediate the function of TAZ in cell growth and epithelial-mesenchymal transition. *J Biol Chem*, **284(20)**, 13355-13362.

Zhang, J., Smolen, G.A., Haber, D.A. (2008a) Negative regulation of YAP by LATS1 underscores evolutionary conservation of the Drosophila Hippo pathway. *Cancer Res*, **68(8)**, 2789-2794.

Zhang, L., Ren, F., Zhang, Q., Chen, Y., Wang, B., Jiang, J. (2008b) The TEAD/TEF family of transcription factor Scalloped mediates Hippo signaling in organ size control. *Dev Cell*, **14(3)**, 377-387.

Zhao, B., Wei, X., Li, W., Udan, R.S., Yang, Q., Kim, J., Xie, J., Ikenoue, T., Yu, J., Li, L., Zheng, P., Ye, K., Chinnaiyan, A., Halder, G., Lai, Z.C., Guan, K.L. (2007) Inactivation of YAP oncoprotein by the Hippo pathway is involved in cell contact inhibition and tissue growth control. *Genes Dev*, **21(21)**, 2747-2761.

Zhao, B., Ye, X., Yu, J., Li, L., Li, W., Li, S., Yu, J., Lin, J.D., Wang, C.Y., Chinnaiyan, A.M., Lai, Z.C, Guan, K.L. (2008) TEAD mediates YAP-dependent gene induction and growth control. *Genes Dev*, **22(14)**, 1962-1971.

Zhao, B., Kim, J., Ye, X., Lai, Z.C., Guan, K.L. (2009) Both TEAD-binding and WW domains are required for the growth stimulation and oncogenic transformation activity of yes-associated protein. *Cancer Res*, **69(3)**, 1089-1098.

Zhao, B., Li, L., Lei, Q., Guan K.L. (2010) The Hippo−YAP pathway in organ size control and tumorigenesis: an updated version. *Genes Dev*, **24(9)**, 862-874.

Zhou, D., Conrad, C., Xia, F., Park, J.S., Payer, B., Yin, Y., Lauwers, G.Y., Thasler, W., Lee, J.T., Avruch, J., Bardeesy, N. (2009) Mst1 and Mst2 maintain hepatocyte quiescence and suppress hepatocellular carcinoma development through inactivation of the Yap1 oncogene. *Cancer Cell*, **16(5)**, 425-438.